HAPS BASED INTEGRATED SPACE AIR GROUND NETWORKS WITH HYBRID FSO/RF COMMUNICATION

M.Tech. Thesis

By
MARRAPU ARAVIND

DEPARTMENT OF ELECTRICAL ENGINEERING
INDIAN INSTITUTE OF TECHNOLOGY INDORE
JUNE 2022

HAPS BASED INTEGRATED SPACE AIR GROUND NETWORKS WITH HYBRID FSO/RF COMMUNICATION

A THESIS

Submitted in partial fulfillment of the
requirements for the award of the degree
of
Master of Technology

by
MARRAPU ARAVIND

DEPARTMENT OF ELECTRICAL ENGINEERING
INDIAN INSTITUTE OF TECHNOLOGY INDORE
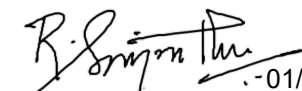### JUNE 2022

INDIAN INSTITUTE OF TECHNOLOGY INDORE

CANDIDATE'S DECLARATION

I hereby certify that the work which is being presented in the thesis entitled **HAPS BASED INTEGRATED SPACE AIR GROUND NETWORKS WITH HYBRID FSO/RF COMMUNICATION** in the partial fulfillment of the requirements for the award of the degree of **MASTER OF TECHNOLOGY** and submitted in the **DEPARTMENT OF ELECTRICAL ENGINEERING, Indian Institute of Technology Indore**, is an authentic record of my own work carried out during the time period from August 2020 to June 2022 under the supervision of **Dr. Swaminathan Ramabadran, Assistant Professor at Indian Institute of Technology Indore**.
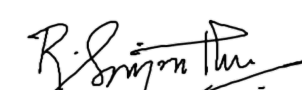
The matter presented in this thesis has not been submitted by me for the award of any other degree of this or any other institute.
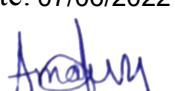
01/06/2022
Signature of the student with date
MARRAPU ARAVIND

This is to certify that the above statement made by the candidate is correct to the best of my/our knowledge.

.-01/06/2022
Signature of the Supervisor of
M.Tech. thesis (with date)
Dr. SWAMINATHAN RAMABADRAN

MARRAPU ARAVIND has successfully given his/her M.Tech. Oral Examination held on **07/06/2022**.

Signature(s) of Supervisor(s) of M.Tech. thesis
Date: 07/06/2022

Convener, DPGC
Date: 07/06/2022

Amod C. Umarikar
Signature of PSPC Member #1
Date: 07/06/2022

Signature of PSPC Member #2
Date: 7/6/2022

Acknowledgments

Abstract

Due to its unique characteristics, free space optics (FSO) communication has gained major importance in providing gigabit capacity links. However, detrimental effects of the transmission medium, such as air turbulence-induced fading, wind, and so on, limit its performance. To improve the performance of FSO communication, it is important to backup with stable radio frequency (RF) links. Future satellite communication (SATCOM) systems could benefit from the integration of FSO and RF technologies. In this respect, the current research provides two unique system models for high-altitude platform station (HAPS)-based uplink and downlink relaying using both FSO and RF links. Further, the obtained closed-form expressions for average symbol error rate (SER) and outage probability are validated using Monte Carlo simulation results. Finally, various interesting inferences have been reported using the obtained performance metrics.

Contents

List of Figures

Chapter 1

Introduction

1.1 Introduction

According to the natural catastrophe report, 396 natural disasters struck the world in 2019, affecting more than 95 million people. Furthermore, it has been reported that Asia has been the site of more than 40% of all natural disasters. As a result, installing more satellites and increasing the monitoring frequency, observation area, and resolution of satellite pictures is vital for India and other Asian countries to avoid disasters. This necessitates large communication capacities and reliable communication links in satellite communication (SATCOM) systems, ushering in a new era for SAGIN and optical-space-based communication [8].

The HAPS (High-Altitude Platform Station) or HAPS (High-Altitude Pseudo-Satellite) is an aerial vehicle that flies above the clouds, often at altitudes of 17 to 25 kilometres, where atmospheric influence on an optical beam is less severe than directly above ground. HAPS has several advantages over satellites, including being easier and faster to install, having lower operational costs, and requiring less maintenance. HAPS can act as a relay station between the satellite and the ground station, increasing the performance of satellite-to-ground station and ground station-to-satellite communication links. The majority of SATCOM systems presently use radio frequency (RF) lines with limited data rates of a few hundred megabits per second (Mbps). There has been a surge of interest in research and development of free space optics (FSO) communications between GS and satellites in recent years, which can give significantly faster data rates, up to terabits per second [13].

Because FSO only allows for high data rates for short-range transmission, the ground-station to satellite FSO link's performance is limited by fading induced by atmospheric tur-

bulence. The FSO system uses a relaying strategy to mitigate atmospheric turbulence, which results in a little boost in system performance. Because the ground station to HAPS link is more susceptible to atmospheric turbulence, it is necessary to back up the high capacity FSO link with a dependable RF link to provide a smooth hybrid FSO/RF communication. However, only FSO link is used for satellite-to-HAPS link as HAPS are located in a cloud-free atmospheric altitude and reliability is not a major concern [19].

1.2 Literature Review

The space-air-ground integrated network (SAGIN) has gained a lot of interest from academics and industry because it uses modern information network technology to connect space, air, and ground network elements. More and more organisations, such as the Global Information Grid (GIG) Oneweb and SpaceX, have started initiatives on SAGIN in recent years [10]. SAGIN can be utilised in a variety of practical domains, including earth observation and mapping, intelligent transportation systems (ITS), military missions, disaster relief, and so on, due to its inherent benefits in terms of vast coverage, high throughput, and great durability. Satellites, in particular, can provide seamless connectivity to rural, ocean, and mountain areas, while air segment networks can boost capacity in covered areas with high service demands and densely distributed ground segment systems can provide high data rate access. Integration of these network segments would provide numerous advantages for future 6G wireless communication. In [22] and [18], the performance of dual-hop (DH) relay-assisted FSO and hybrid FSO/RF communication was investigated for terrestrial communication. [12] examined the performance of a hybrid satellite-terrestrial FSO cooperative link using a satellite RF link and a terrestrial FSO link. In the SATCOM context, however, there are just a few publications that look into single-hop (SH) FSO communication between the satellite and the ground station. A performance study of an FSO-based downlink SATCOM system with spatial diversity was carried out in [15] over fading channels caused by Gamma-Gamma turbulence. Closed-form expressions were only available for the outage probability and not the average bit error rate (BER). In addition, the BER of numerous modulation schemes for SH FSO-based uplink and downlink SATCOM systems was assessed in [8]. To our knowledge, performance analysis of DH HAPS-based SATCOM system has not been provided considering multiple-HAPS and end-to-end uplink and downlink scenarios

over generalized FSO and RF channel distributions.

1.3   Motivations and Contributions

1.3.1   Chapter 2

The motivations behind the work in Chapter 2 are summarized as follows:

- In the case of uplink scenario, the performance of FSO link over Malaga fading channel for decode-and-forward (DF) relaying in the presence of both direct link and relay link has not been investigated in the existing literature to the best of our knowledge.

- Furthermore, performance analysis of the system model consisting of multiple HAPS has not been done studied yet.

- In particular, the performance analysis in [15] was reported considering Gamma-Gamma distribution. Therefore, there is a need to analyze the performance of the channel considering Malaga distribution.

The contributions of the work in Chapter 2 are summarized as follows:

- The closed-form expressions for performance metrics such as outage probability and symbol error rate (SER) of the proposed system model are derived.

- The Monte Carlo simulations are also carried out to validate the derived closed-form expressions.

1.3.2   Chapter 3

The motivations behind the work in Chapter 3 are summarized as follows:

- In the case of uplink scenario, the performance of hybrid FSO/RF link over Malaga fading channel for DF relaying in the presence of both direct link and relay link has not been investigated in the existing literature to the best of our knowledge.

- Furthermore, performance analysis of the system model consisting of multiple HAPS has not been done studied yet.

- There is a need to derive the closed-form expressions for the outage probability and SER in order to perform exact analysis.

The contributions of the work in Chapter 3 are summarized as follows:

- The closed-form expressions for performance metrics such as outage probability and SER of the proposed system model over Malaga fading channels are derived.

- Finally, Monte Carlo simulations are performed to validate the derived performance metrics.

1.3.3 Chapter 4

The motivations behind the work in Chapter 4 are summarized as follows:

- The existing literature lacks in deriving the exact outage probability and SER expressions for end-to-end communication i.e from ground station to satellite (uplink) and thereby to ground station (downlink).

- The existing literature also lacks performance analysis of system model consisting of multiple HAPS for end-to-end communication scenario.

The contributions of the work in Chapter 4 are summarized as follows:

- The closed-form expressions for performance metrics such as outage probability and SER of the proposed system model are derived.

- The Monte Carlo simulations are also carried out to validate the derived closed-form expressions.

1.4   Organization of the Thesis

The rest of this thesis is organized as follows: In Chapter 2, the system model for uplink scenario using FSO link along with HAPS as relay is discussed. Further, in chapter 3, the performance analysis of the system model for uplink scenario using hybrid FSO/RF link with HAPS acting as relay is discussed. Chapter 4 shows the performance analysis of the end to end system model i.e combination of both uplink and downlink scenarios is discussed. Finally, chapter 5 includes the conclusion and scope of the future work of this thesis.

Chapter 2

Performance Analysis of multiple HAPS-based Uplink FSO Communication

2.1 Introduction

This chapter describes a dual-hop (DH) uplink communication i.e from ground station (S) to satellite (D) as system model with HAPS (R) acting as relay between S and D. In the proposed system model, we employed one ground station, relays, and one satellite. Further, we assume all receiver nodes know the full channel state information (CSI) of all the links. Out of multiple relays, one is selected based on the relay selection scheme. Here, partial relay selection (PRS) is considered in our work. In the PRS scheme, only CSI between source-to-relay links are required. One relay is selected out of multiple relays based on the instantaneous signal-to-noise ratio (SNR) between source-to-relay links. The performance of this proposed system is analyzed by deriving the exact outage probability and symbol error rate (SER) expressions over Malaga fading channels [12].

2.2 Organisation of chapter

The rest of the chapter is organized as follows: The system model for uplink communication using FSO link and HAPS as a relay has been discussed in Section 2.3. Section 2.4 provides the closed-form expressions for outage probability and SER over Malaga fading

channels. Furthermore, numerical results and inferences are given in Section 2.5. Finally, the concluding remarks are given in Section 2.6.

2.3   System Model

Let us consider an uplink model as shown in Figure 2.1, where a ground station (S) intends to transmit the signal to satellite with the help of a single relay, which is selected out of N number of relays based on PRS scheme. Here out of N relays, one relay is selected based on the instantaneous SNR between S (Source) $\rightarrow R_n(Relay)$ links, where, $n = 1, 2, ...N$. Here the data transmission takes place in two phases, and we assume symbol by symbol transmission [14]. Let $h_{i,j}$ represents the independent Malaga fading channel coefficient between nodes i and j where, $i \neq j$, $i \in \{S, R_n\}$, $j \in \{R_n, D\}$. At the beginning of the transmission, the source node selects one relay based on the instantaneous SNR of source-to-relay links.
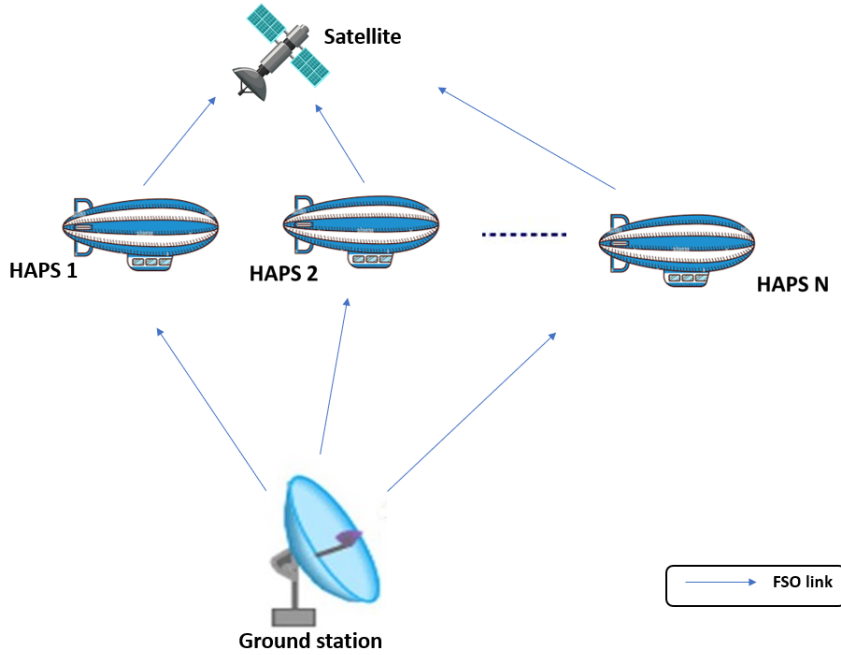
Figure 2.1: System Model

Two-phase orthogonal transmission is used in the considered system model. During the first phase of the uplink scenario, S transmits the information signal to R across the FSO link. R delivers the decoded information signal to D over the FSO link during the second or orthogonal phase transmission. One relay is chosen based on the value of the instantaneous

6

SNR of S-R links [5]. It is not necessary to check the SNR of the FSO link at regular intervals because the FSO channel varies on the order of millions of symbol intervals [1]. In addition, a sub-carrier intensity modulation based M-ary phase-shift-keying (SIM-MPSK) scheme is assumed.

First Phase:

The received signals at HAPS relay $R_1, R_2...R_n$ are given by

$$y_1 = h_{SR_1} \, x_1 + n_1 \tag{2.1}$$

$$y_2 = h_{SR_2} \, x_1 + n_1 \tag{2.2}$$

$$.$$
$$.$$
$$.$$

$$y_n = h_{SR_n} \, x_1 + n_1 \tag{2.3}$$

where n_1 denote the additive white Gaussian noise (AWGN) with zero mean and variance σ^2, and $h_{SR_1}, h_{SR_2}....h_{SR_n}$ are the fading channel coefficients for S-R link.

Second phase:

The received signal at D in the second phase can be expressed as

$$y_D = h_{R_n D} \, x_2 + n_2 \tag{2.4}$$

where n_2 represent the AWGN at D with zero mean and variance σ^2, and $h_{R_n D}$ is the fading channel coefficient for R-D link and index n value can be any value from 1 to n depending upon which relay is selected.

2.3.1 FSO channel model

According to the Malaga distribution, three components of the detected field at the receiver are statistically accounted for: (a) dictates the LOS component (b) denotes the coupled to LOS component that is scattered by the eddies on the propagation axis (c) the third component, which is scattered to the receiver by off-axis eddies. The probability density function (PDF) of irradiance I_a FSO link is modeled using Malaga distribution and is given by,

$$f_{I_a}(I_a) = A \sum_{m=1}^{\beta} a_m I_a^{\frac{\alpha+m}{2}-1} K_{\alpha-m}\left(2\sqrt{\frac{\alpha\beta I_a}{\rho\beta+\Omega^1}}\right) \tag{2.5}$$

7

where $b_m = a_m(\frac{\alpha\beta}{\rho\beta+\Omega^1})^{-(\alpha+m)/2}$, $a_m = \binom{\beta-1}{m-1}\frac{(\rho\beta+\Omega^1)^{1-m/2}}{m!}(\frac{\Omega^1}{\rho})^{m-1}(\frac{\alpha}{\beta})^{m/2}$,

$A = \frac{2\alpha^{\alpha/2}}{(\rho^{1+\alpha/2})\Gamma(\alpha)}(\frac{\rho\beta}{\rho\beta+\Omega^1})^{\beta+\alpha/2}$, α is a positive parameter related to the effective number of large-scale cells of the scattering process, and β is the amount of fading parameter and is a natural number. The radial displacement ρ between the beam center and detector center, which induces pointing error, has been modeled using Rayleigh distribution. The amount of the received power collected at the receiver aperture of radius a can be expressed in Gaussian form as

$$I_p = A_o \exp\left(-\frac{2\rho^2}{w_{leq}}\right) \tag{2.6}$$

where $A_o = erf^2(v)$, $v = \frac{\sqrt{\pi}a}{\sqrt{2}w_L}$ and $w_{leq} = \frac{w_L^2\sqrt{\pi}erf(v)}{2v\exp(-v^2)}$. Here a is radius of detector aperture, w_l is beam waist and $erf(.)$ is the error function. It is to be noted that the radial displacement ρ follows the Rayleigh distribution and using the random variable transformation, the PDF of pointing error is expressed as [2]

$$f_{I_p}(I_p) = \frac{g^2}{A_o^{g^2}}I_p^{(g^2-1)} \tag{2.7}$$

where $g = \frac{w_{leq}}{2\sigma_s}$, represents the pointing error coefficient and σ_s is the jitter standard deviation. Beers Lambert Law [15] defines the atmospheric path loss of an optical link as $I_l = exp(-\alpha_j L)$ where α_j is the attenuation coefficient which depends on weather conditions and link distance L. The combined atmospheric channel state of FSO link includes irradiance, pointing errors and path loss and is written as $I = I_a I_p I_l$. The combined channel PDF is given by

$$f_I(I) = \int_{I/I_l A_0}^{\infty} f_{I_a}(I_a) f_{I/I_a}(I/I_a)\, dI_a \tag{2.8}$$

$$= \int_{I/I_l A_0}^{\infty} f_{I_a}(I_a)\frac{1}{I_a I_l}f_p(\frac{I}{I_a I_l})\, dI_a \tag{2.9}$$

By substituting (2.5) and (2.7) in (2.9) the integral gives

$$f_I(I) = \frac{A\rho^2}{2I}\sum_{m=1}^{\beta} b_m G_{1,3}^{3,0}\left(\frac{\alpha\beta I}{(\rho\beta+\Omega^1)I_l A_0}\,\middle|\,\begin{matrix}g^2+1\\g^2,\alpha,m\end{matrix}\right) \tag{2.10}$$

Instanteneous SNR is given by, $\gamma = \frac{n_e I}{N_0}$ and average SNR is obtained by $E[\gamma]$ and it is given by $\gamma_{avg} = \frac{n_e E[I]}{N_0}$. Here $E[I]$ represents expectation of I, n_e is effective photoelectric conversion rate and N_0 is noise power(AWGN). Average SNR can also be written as $\gamma_{avg} = \frac{I_l A_0(\rho+\Omega^1)g^2}{(1+g^2)N_0}$. By using random variable transformation, the PDF of instantaneous SNR of FSO link un-

dergoing Malaga fading considering both IM/DD and HD technique is obtained as

$$f_{\gamma_{ii}^f}(\gamma_{ii}) = D_1 \sum_{m=1}^{\beta} \frac{b_m}{\gamma_{ii}} G_{1,3}^{3,0} \left(B_1 \left(\frac{\gamma_{ii}}{\gamma_{avg}} \right)^{\frac{1}{r}} \middle| \begin{matrix} g^2+1 \\ g^2, \alpha_{ii}, m_{ii} \end{matrix} \right) d\gamma_{ii} \tag{2.11}$$

where $D_1 = \frac{A\rho^2}{2^r}$, $B_1 = \frac{\alpha\beta(\rho+\Omega^1)g^2}{(\rho\beta+\Omega^1)(g^2+1)}$, r denotes the unifying parameter which takes value $r=1$ for HD detection, and $r=2$ for IM/DD detection and ii={SR,RD}.

2.4 Performance Analysis

2.4.1 Outage probability of a FSO link

The CDF is obtained by integrating PDF over limits 0 and γ, which is given by

$$F_{\gamma_{ii}^f}(\gamma_{ii}) = \int_0^{\gamma_{ii}} f_{\gamma_{ii}^f}(t)\, dt \tag{2.12}$$

After substituting (2.11) in (2.12), we get

$$F_{\gamma_{ii}^f}(\gamma_{ii}) = \int_0^{\gamma_{ii}} D_1 \sum_{m=1}^{\beta} \frac{b_m}{t} G_{1,3}^{3,0} \left(B_1 \left(\frac{t}{\gamma_{avg}} \right)^{\frac{1}{r}} \middle| \begin{matrix} g^2+1 \\ g^2, \alpha_{ii}, m_{ii} \end{matrix} \right) dt \tag{2.13}$$

Simplifying above expression using the [11, eq.(07.34.21.0084.01)], final outage probability expression for FSO link can be written as

$$F_{\gamma_{ii}^f}(\gamma_{th}) = D_1 \sum_{m=1}^{\beta} c_m G_{r+1,3r+1}^{3r,1} \left(\frac{E\gamma_{th}}{\gamma_{avg}} \middle| \begin{matrix} 1,k_1 \\ k_2,0 \end{matrix} \right) \tag{2.14}$$

where $E = \frac{B_1^r}{2^r}$, $k_1 = [\frac{g^2+1}{r} ..... \frac{g^2+r}{r}]$, $k_2 = [\frac{g^2}{r} ..... \frac{g^2+r-1}{r}, \frac{\alpha}{r} .... \frac{\alpha+r-1}{\alpha}, \frac{m}{r} ... \frac{m+r-1}{r}]$, and $c_m = b_m r^{\alpha+m-1}$.

2.4.2 Outage probability analysis of uplink using single HAPS

The outage probability of DH link is given by

$$P_0^{DH} = 1 - \{(1-P_0^{SR})(1-P_0^{RD})\}$$
$$= P_0^{SR} + P_0^{RD} - P_0^{SR}P_0^{RD} \tag{2.15}$$

where $P_0^{SR} = F_{\gamma_{SR}^f}(\gamma_{SR})$ and $P_0^{RD} = F_{\gamma_{RD}^f}(\gamma_{RD})$.

From the (2.14) P_0^{SR} can be obtained, i.e.

$$P_0^{SR} = D_1 \sum_{m=1}^{\beta} c_m G_{r+1,3r+1}^{3r,1} \left(\frac{E\gamma_{th}}{\gamma_{avg}} \middle| \begin{matrix} 1,k_1 \\ k_2,0 \end{matrix} \right) \tag{2.16}$$

P_0^{RD} is almost negligible due to negligible atmospheric affects in relay to destination region. The final expression for DH outage probability with single HAPS is majorly dependent on S-R link outage probability. After substituting P_0^{SR} and P_0^{RD} values in (2.16) the final expression will be

$$P_0^{DH} = D_1 \sum_{m=1}^{\beta} c_m G_{r+1,3r+1}^{3r,1} \left(\frac{E\gamma_{th}}{\gamma_{avg}} \middle| \begin{array}{l} 1,k_1 \\ k_2,0 \end{array} \right) \qquad (2.17)$$

2.4.3 Outage probability analysis of uplink using multiple HAPS

The outage probability of DH link with multiple HAPS is obtained when all the N links i.e. SR_1 and $SR_2....SR_n$ are in outage along with the $R-D$ link and it is mathematically represented as

$$P_1^{DH} = P\left(max(\gamma_{SR_1}, \gamma_{SR_2}....\gamma_{SR_n}) < \gamma_{th} \cap \gamma_{RD} < \gamma_{th}\right) \qquad (2.18)$$

This can also be written as

$$P_1^{DH} = 1 - \{(1-P_1^{SR})(1-P_1^{RD})\}$$

$$P_1^{DH} = P_1^{SR} + P_1^{RD} - P_1^{SR}P_1^{RD} \qquad (2.19)$$

where $P_1^{SR} = [F_{\gamma_{SR_1}^f}(\gamma_{SR_1})F_{\gamma_{SR_2}^f}(\gamma_{SR_2})....F_{\gamma_{SR_n}^f}(\gamma_{SR_n})]$ and $P_1^{RD} = F_{\gamma_{RD}^f}(\gamma_{RD})$. From the (2.16), P_1^{SR} can be obtained as

$$P_1^{SR} = \left[D_1 \sum_{m=1}^{\beta} c_m G_{r+1,3r+1}^{3r,1} \left(\frac{E\gamma_{th}}{\gamma_{avg}} \middle| \begin{array}{l} 1,k1 \\ k2,0 \end{array} \right) \right]^N \qquad (2.20)$$

P_1^{RD} is negligible (almost zero). The final expression for DH outage probability with multiple HAPS is majorly dependent on S-R link outage probability. After substituting P_1^{SR} and P_1^{RD} values in (2.19). The final expression will be

$$P_1^{DH} = \left[D_1 \sum_{m=1}^{\beta} c_m G_{r+1,3r+1}^{3r,1} \left(\frac{E\gamma_{th}}{\gamma_{avg}} \middle| \begin{array}{l} 1,k1 \\ k2,0 \end{array} \right) \right]^N \qquad (2.21)$$

2.4.4 Symbol error rate of a FSO link

The conditional SER of MPSK signalling based on the instantaneous SNR of given link is

$$p(e/\gamma_{ii}) = \frac{A}{2}\text{erfc}\left(\sqrt{\gamma_{ii}}B\right) \qquad (2.22)$$

where $A = 1$ when modulation order $M = 2$ i.e. binary phase-shift keying (BPSK), $A = 2$ when $M > 2$, $B = \sin(\pi/M)$, and $\text{erfc}(\cdot)$ denotes the complementary error function. Using the relation between $\text{erfc}(\cdot)$ and Meijer G-function [11, eq.(07.34.03.0619.01)], the conditional SER can also be written in terms of Meijer G-function and is given by

$$p(e/\gamma_{ii}) = \frac{A}{2\sqrt{\pi}} G_{1,2}^{2,0}\left(B^2 \gamma_{ii} \,\middle|\, \begin{matrix} 1 \\ \alpha, \beta \end{matrix} \right). \tag{2.23}$$

The conditional SER can also be expressed in terms of Maclaurin series expansion and is given by

$$p(e/\gamma_{ii}) = \frac{A}{2}\left\{ 1 - \frac{2}{\sqrt{\pi}} \sum_{k=0}^{\infty} \frac{(-1)^k (\gamma_{ii})^{\frac{2k+1}{2}} B^{2k+1}}{k!(2k+1)} \right\} \tag{2.24}$$

The average SER of FSO link is obtained by integrating the conditional SER over the PDF of instantaneous SNR of FSO link i.e.

$$P_e = \int_0^{\infty} p(e/\gamma_{ii}) f_{\gamma_{ii}^f}(\gamma_{ii})\, d\gamma_{ii} \tag{2.25}$$

After substituting the corresponding terms in (2.25), the average SER is given by

$$P_e = \int_0^{\infty} \frac{A}{2\sqrt{\pi}} G_{1,2}^{2,0}\left(B^2 \gamma_{ii} \,\middle|\, \begin{matrix} 1 \\ \alpha, \beta \end{matrix} \right) D_1 \sum_{m=1}^{\beta} \frac{b_m}{\gamma_{ii}} G_{1,3}^{3,0}\left(B_1 \left(\frac{\gamma_{ii}}{\gamma_{avg}}\right)^{\frac{1}{r}} \,\middle|\, \begin{matrix} g^2 + 1 \\ g^2, \alpha_{ii}, m_{ii} \end{matrix} \right) d\gamma_{ii} \tag{2.26}$$

Using [11, eq. 07.34.21.0013.01] and simplifying above integral gives average SER of FSO link, which is given by

$$P_e^{FSO} = D_2 \sum_{m=1}^{\beta} c_m G_{r+2,3r+1}^{3r,2}\left(\frac{E}{\gamma_{avg}} \,\middle|\, \begin{matrix} 1, 0.5, k_1 \\ k_2, 0 \end{matrix} \right) \tag{2.27}$$

where $D_2 = \frac{A\rho^2}{2^r (2\pi)^{r-1}}$.

2.4.5 Average SER of DH uplink FSO communication with single HAPS

The conditional SER of S-R-D link during uplink can be written as

$$P_{e_{SRD}}(\gamma_{SR}, \gamma_{RD}) = P_e(\gamma_{SR}) + P_e(\gamma_{RD}) - P_e(\gamma_{SR}) P_e(\gamma_{RD}) \tag{2.28}$$

After averaging (2.28) over the PDFs of the instantaneous SNR of FSO link, the average SER is given by

$$P_e^{SRD} = P_e^{SR} + P_e^{RD} - P_e^{SR}P_e^{RD} \tag{2.29}$$

where P_e^{SR} denotes the average SER of FSO link, which is given in (2.27)

$$P_e^{SR} = D_2 \sum_{m=1}^{\beta} c_m G_{r+2,3r+1}^{3r,2} \left(\frac{E}{\gamma_{avg}} \middle| \begin{array}{c} 1,0.5,k_1 \\ k_2,0 \end{array} \right) \tag{2.30}$$

Since R-D link behaves as an AWGN channel due to negligible distortions, the average SER expression can be written as

$$p_e^{RD} = \frac{A}{2}\text{erfc}\left(\sqrt{\gamma_{avg}}B\right) \tag{2.31}$$

The final expression for SER is obtained by substituting (2.30) and (2.31) in (2.29).

2.4.6   Average SER of uplink using FSO link with multiple HAPS

While calculating average SER for multiple HAPS scenario, the only thing that changes from single HAPS scenario is S-R part. In multiple HAPS case with N links, the PDF calculation is quite different.

The CDF in the case of N links is given by

$$F_\gamma(\gamma) = P(max(\gamma_{SR_1}, \gamma_{SR_2}....\gamma_{SR_n}) < \gamma_{th}) \tag{2.32}$$

$$F_\gamma(\gamma) = P(\gamma_{SR_1} < \gamma_{th})P(\gamma_{SR_2} < \gamma_{th}).....P(\gamma_{SR_n} < \gamma_{th}) \tag{2.33}$$

$$F_\gamma(\gamma) = F_{\gamma_{SR_1}}(\gamma)F_{\gamma_{SR_2}}(\gamma).....F_{\gamma_{SR_n}}(\gamma) \tag{2.34}$$

Now PDF is obtained by differentiating the CDF expression

$$f_\gamma(\gamma) = [f_{\gamma_{SR_1}}(\gamma)F_{\gamma_{SR_2}}(\gamma)...F_{\gamma_{SR_n}}(\gamma)] + [f_{\gamma_{SR_2}}(\gamma)F_{\gamma_{SR_1}}(\gamma)...F_{\gamma_{SR_n}}(\gamma)] + ...$$
$$[f_{\gamma_{SR_n}}(\gamma)F_{\gamma_{SR_1}}(\gamma)...F_{\gamma_{SR_{n-1}}}(\gamma)] \tag{2.35}$$

We have assumed that all these links are identical, so $f_{\gamma_{SR_1}}(\gamma) = f_{\gamma_{SR_2}}(\gamma) = f_{\gamma_{SR_n}}(\gamma) = f_{\gamma_{SR}}(\gamma)$ and $F_{\gamma_{SR_1}}(\gamma) = F_{\gamma_{SR_2}}(\gamma) = F_{\gamma_{SR_n}}(\gamma) = F_{\gamma_{SR}}(\gamma)$

Finally, PDF in the case of multiple HAPS with N links can be written as

$$f_\gamma(\gamma) = N \times f_{\gamma_{SR}}(\gamma_{SR})[F_{\gamma_{SR}}(\gamma_{SR})]^{N-1} \tag{2.36}$$

The average SER of this system model is given by

$$P_e^{SR} = N \times \int_0^\infty P(e/\gamma_{SR})f_{\gamma_{SR}}(\gamma_{SR})[F_{\gamma_{SR}}(\gamma_{SR})]^{N-1} \, d\gamma_{SR} \tag{2.37}$$

Because of the constraints in the calculation of average SER of generalized N links case, we are considering the special case of $N = 2$ and it is given by

$$P_e^{SR} = \int_0^\infty 2P(e/\gamma_{SR}) f_{\gamma_{SR}}(\gamma_{SR}) F_{\gamma_{SR}}(\gamma_{SR}) \, d\gamma_{SR} \tag{2.38}$$

By substituting the (2.11),(2.14) and (2.23) in (2.41), we get

$$P_e^{SR} = \int_0^\infty \frac{A}{2\sqrt{\pi}} G_{1,2}^{2,0} \left(B^2 \gamma_{SR} \,\middle|\, \begin{matrix} 1 \\ \alpha, \beta \end{matrix} \right) D_1 \sum_{m=1}^\beta \frac{b_m}{\gamma_{SR}} G_{1,3}^{3,0} \left(B_1 \left(\frac{\gamma_{SR}}{\gamma_{avg}} \right)^{\frac{1}{r}} \,\middle|\, \begin{matrix} g^2 + 1 \\ g^2, \alpha_{ii}, m_{ii} \end{matrix} \right)$$
$$\times D_1 \sum_{m=1}^\beta c_m G_{r+1,3r+1}^{3r,1} \left(\frac{E \gamma_{SR}}{\gamma_{avg}} \,\middle|\, \begin{matrix} 1, k_1 \\ k_2, 0 \end{matrix} \right) d\gamma_{SR} \tag{2.39}$$

From equation [11, eq. 07.34.17.0013.01], $f_{\gamma_{SR}}(\gamma_{SR})$ can also written as

$$f_{\gamma_{SR}}(\gamma_{SR}) = D_1 \sum_{m_1=1}^\beta \frac{c_{m_1}}{\gamma_{SR}} G_{r,3r}^{3r,0} \left(\frac{E \gamma_{SR}}{\gamma_{avg}} \,\middle|\, \begin{matrix} k_1 \\ k_2 \end{matrix} \right) \tag{2.40}$$

where $c_{m_1} = b_m r^{\alpha+m-1}$. Now replacing the expression of $f_{\gamma_{SR}}(\gamma_{SR})$ in (2.39) with (2.40) gives

$$P_e^{SR} = \int_0^\infty \frac{A}{2\sqrt{\pi}} G_{1,2}^{2,0} \left(B^2 \gamma_{SR} \,\middle|\, \begin{matrix} 1 \\ \alpha, \beta \end{matrix} \right) D_1 \sum_{m_1=1}^\beta \frac{c_{m_1}}{\gamma_{SR}} G_{r,3r}^{3r,0} \left(\frac{E \gamma_{SR}}{\gamma_{avg}} \,\middle|\, \begin{matrix} k_1 \\ k_2 \end{matrix} \right)$$
$$\times D_1 \sum_{m=1}^\beta c_m G_{r+1,3r+1}^{3r,1} \left(\frac{E \gamma_{SR}}{\gamma_{avg}} \,\middle|\, \begin{matrix} 1, k_1 \\ k_2, 0 \end{matrix} \right) d\gamma_{SR} \tag{2.41}$$

Simplifying the above equation based on [22, eq.07.34.21.0081.01] gives the following expression in terms of bi-variate Meijer G-function

$$P_e^{SR} = \sum_{m=1}^\beta \sum_{m_1=1}^\beta c_m c_{m_1} \frac{A D_1^2}{2\sqrt{\pi}} G_{2,1:r,3r:r+1,3r+1}^{0,2:3r,0:3r,1} \left(\begin{matrix} 1, 0.5 \\ 0 \end{matrix} \,\middle|\, \begin{matrix} k_1 \\ k_{2m_1} \end{matrix} \,\middle|\, \begin{matrix} 1, k_1 \\ k_{2m}, 0 \end{matrix} \,\middle|\, \frac{E}{B^2 \gamma_{avg}}, \frac{E}{B^2 \gamma_{avg}} \right) \tag{2.42}$$

2.5 Numerical Results and Discussions

We will look at the derived closed-form expressions in this section. We also show how different parameters affect outage probability (OP), average SER for the proposed system model. For numerical investigation, we set threshold SNR $\gamma_{th} = 5$ dB, height at which HAPS is located at 20 km, $\lambda = 1.55 \mu m$, $\alpha_{SR} = 2.89$, $\beta_{SR} = 2$, $\alpha_{RD} = 801.6$, $\beta_{RD} = 1024$ and the

parameters considered for making conclusions are pointing error coefficient, wind velocity and zenith angle.
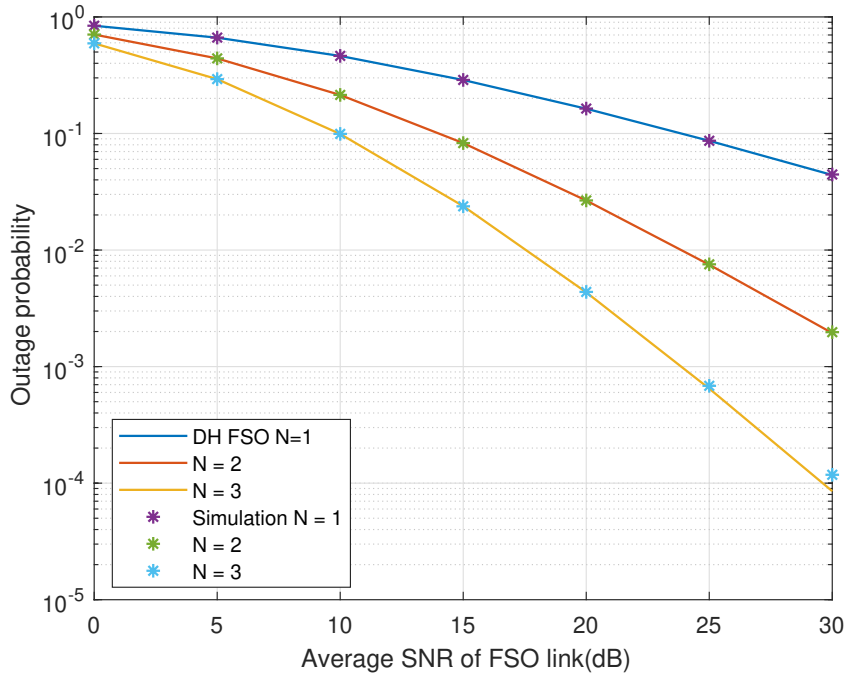
Figure 2.2: OP vs Avg. SNR of FSO link for different values of *N*

Figure 2.2 the impact of the number of relays *N* on the outage probability. We can see from the graph that as the value of *N* increases, the outage performance improves. Because more relays are used in this system, the best relay out of *N* relays can be chosen. The SNRs necessary for the system with *N*=1, *N*=2, and *N*=3 to achieve the outage probability of 10^{-1} are 25 dB, 15 dB, and 10 dB, respectively. Hence, the SNR gains achieved by the system with *N*=2, *N*=3 w.r.t system with *N*=1 are 5 dB, 15 dB. As a result, it has been deduced that as the value of *N* increases, there is much improvement in SNR gain. The outage probability tends to decrease when SNR increases. The reason for this is that as the SNR rises, the signal becomes considerably stronger than the noise.

Figure 2.3: OP vs. Avg. SNR of FSO link for different values of ζ_{SR}

Figure 2.3 shows the impact of value of ζ_{SR} pointing error coefficient on the outage probability of the system model. From the plot, we can observe that with the increase ζ_{SR}, the outage performance improves.Because, increase in pointing error coefficient implies decrease in pointing error. The SNRs required to achieve the outage probability of 10^{-1}, for the system with $\zeta_{SR} = 1$, $\zeta_{SR} = 1.7$, $\zeta_{SR} = 5$ are 30 dB, 25 dB, 24 dB respectively. Thus, the SNR gains achieved by the system with $\zeta_{SR} = 1$ w.r.t system with $\zeta_{SR} = 1.7$, $\zeta_{SR} = 5$ are 5 dB, 6 dB respectively. Thus, it has been deduced that with the increase in value of ζ_{SR} above 1.7, there is not much of a difference in SNR gain.

Figure 2.4: OP vs Avg. SNR of FSO link for different values of w

Figure 2.5: OP vs Avg. SNR of FSO link for different values of θ_p

Figure 2.4 and 2.5 shows the effect of the wind velocity and zenith angle on system model w.r.t outage probability. We can see from both graphs that as the value of w increases, outage probability increases. Similarly, when θ_p rises, outage performance decreases. The

16

reason in case of wind velocity is that as wind velocity increases the irradiance fluctuations increases and therefore, the performance degrades. While in the case of zenith angle, it is directly proportional to link distance i.e. greater the zenith angle, greater the link distance and hence, probability for system in outage increases.
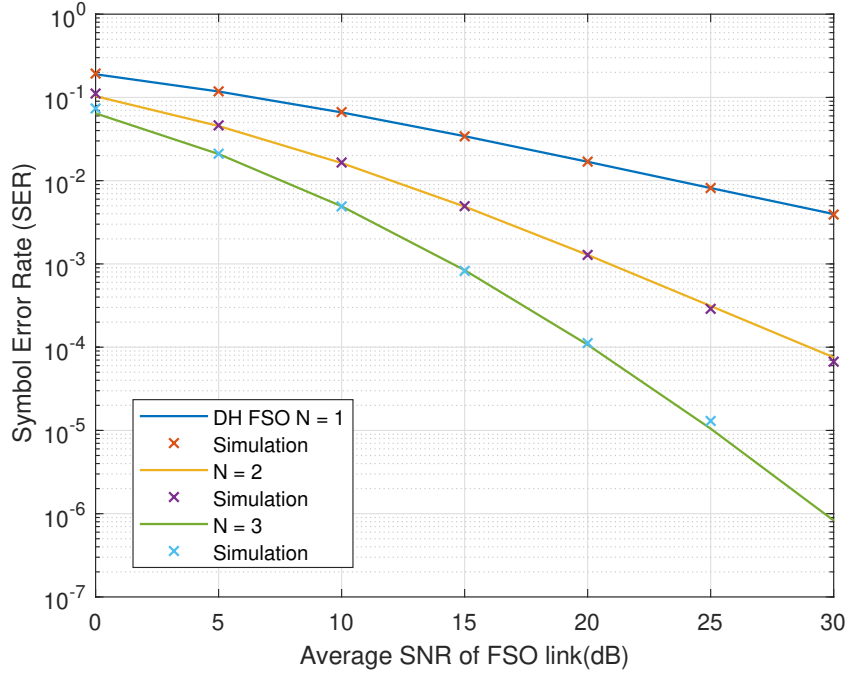
Figure 2.6: SER vs Avg. SNR of FSO link for N links

Figure 2.6 shows the impact of the number of relays in system N on average SER. We can see from the graph that as the value of N increases, the SER performance improves. Because more relays are used in this system, the best relay out of N relays can be chosen. The SNRs necessary for the system with $N=1$, $N=2$, and $N=3$ to achieve the SER of 10^{-2} are 24 dB, 12.5 dB, 7.5 dB, respectively. So, the SNR gains achieved by the system with $N=2$, $N=3$ w.r.t system with $N=1$ are 11.5 dB, 16.5 dB, respectively. As a result, it has been deduced that as the value of N increases, the SNR gain improves significantly. When SNR increases, the SER tends to decrease. The reason for this is that as the SNR increases, the signal becomes considerably stronger than the noise.
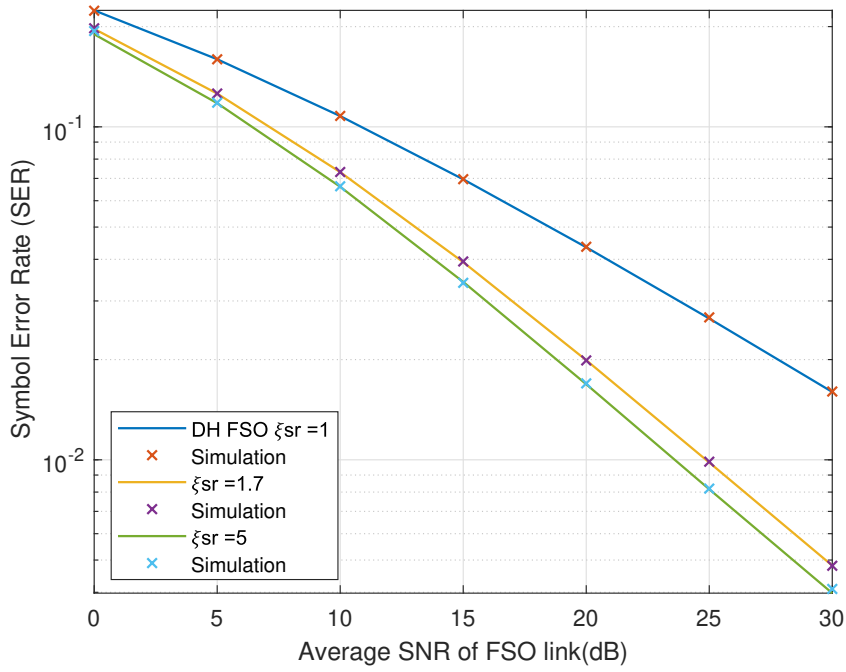
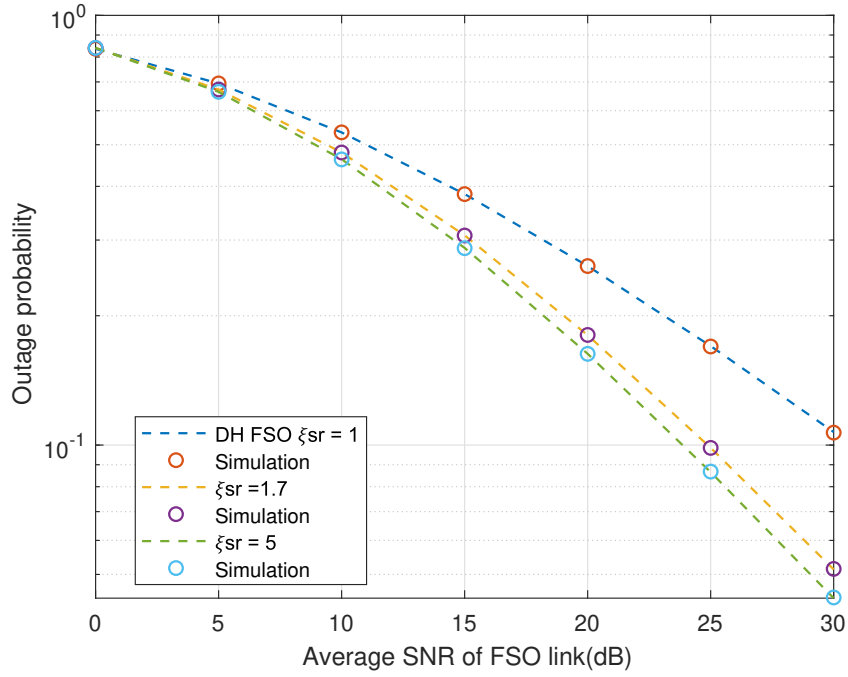Figure 2.7: SER vs. Avg. SNR of FSO link for different values of ζ_{SR}

Figure 2.7 shows the effect of value of pointing error coefficient ζ_{SR} on the average SER. From the plot, we can observe that with the increase in ζ_{SR}, the SER performance improves. Because, increase in pointing error coefficient implies decrease in pointing error. The SNRs required to achieve the average SER of 10^{-1}, for the system with $\zeta_{SR}=1$, $\zeta_{SR}=1.7$, $\zeta_{SR}=5$, are 10 dB,7 dB ,6.5 dB respectively. So, the SNR gains achieved by the system with $\zeta_{SR}=1$ w.r.t system with $\zeta_{SR}=1.7$,$\zeta_{SR}=5$ are 3 dB, 3.5 dB respectively. From this it has been inferred that with the increase in value of ζ_{SR} above 1.7, there is not much of a difference in the SNR gain.

18

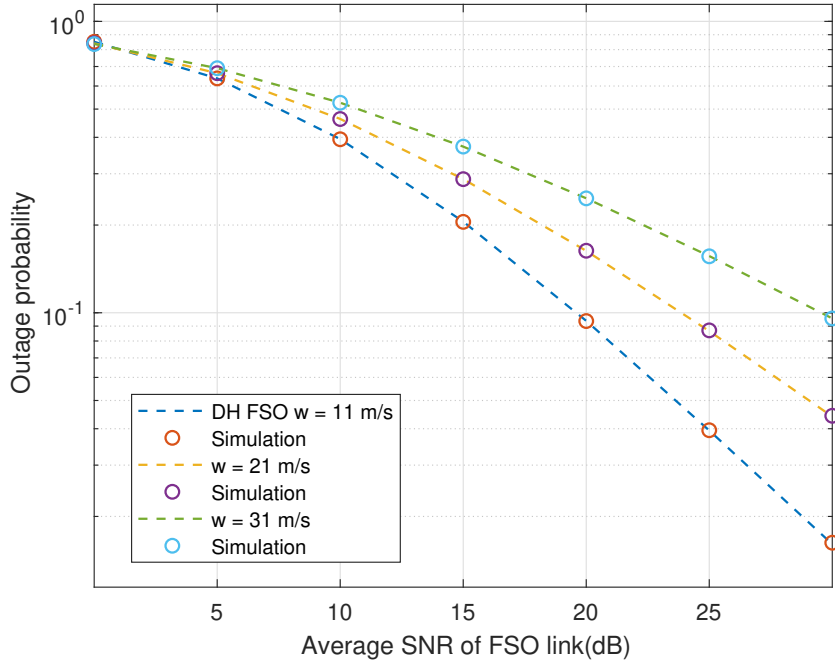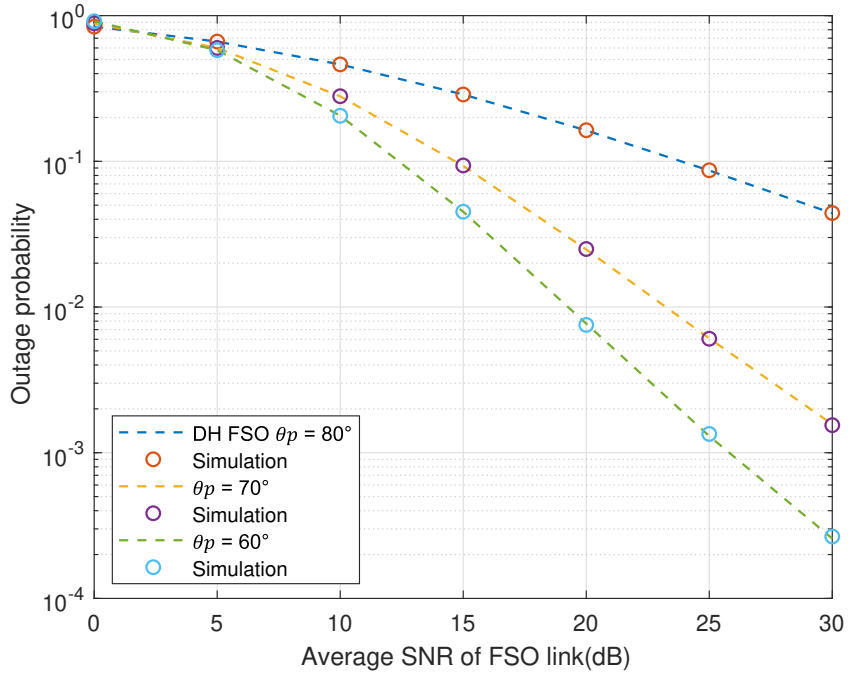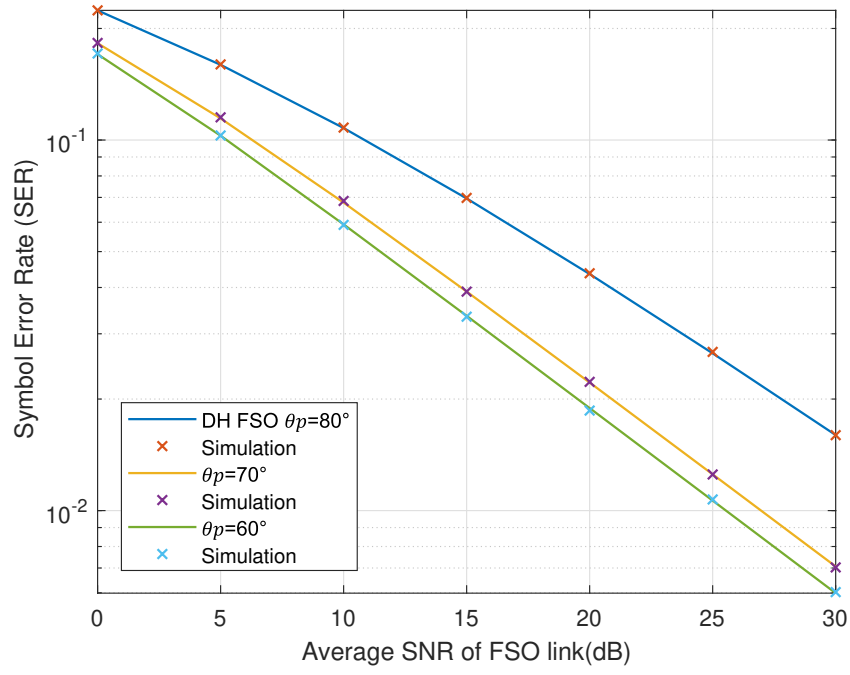Figure 2.8: SER vs Avg. SNR of FSO link for different values of θ_p
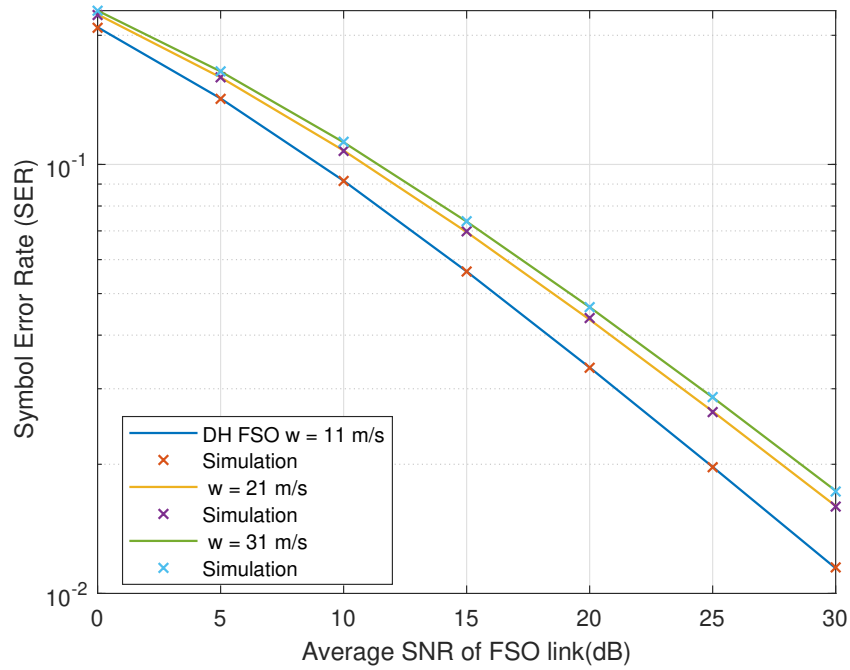
Figure 2.9: SER vs Avg. SNR of FSO link for different values of w

Figure 2.8 and 2.9 show the effect of the wind velocity and zenith angle on average SER. We can see from both graphs that as the value of w and θ_p increases, the SER performance deteriorates. The reason in case of wind velocity is that as wind velocity increases, the

disturbance in atmosphere increases and hence, link performance degrades. While in the case of zenith angle, it is directly proportional to link distance i.e. greater the zenith angle, greater the link distance and thereby, greater the chances for symbol error.

2.6   Conclusions

The performance of DH uplink system with HAPS as relay is investigated in this chapter by deriving the accurate outage probability and average SER expressions in closed-form over Malaga fading channels. In addition, MATLAB is used to compute the derived closed-form expressions for performance metrics [20]. The outage performance of the suggested system model improves as the value of N increases. Furthermore, the system with relay has superior outage performance than the system without relay. Finally, the theoretical outage probability and SER values accord well with the simulated outage probability and SER values obtained from Monte Carlo simulations. As a result, the derived expressions are validated.

Chapter 3

Performance Analysis of multiple HAPS-based Uplink Hybrid FSO/RF Communication

3.1   Introduction

The exact expressions for dual-hop uplink communication using FSO over Malaga fading channels are derived in chapter 2. With that the system performance has been improved compared to the scenario without relay, but there is a scope for further improvement in the system performance. FSO link gets be affected by atmospheric effects such as fog, smog and dust, whereas RF link gets more effected by rain and snow. This complementary behaviour of the two links led to new system model. Therefore, in first phase of communication from S to HAPS, hybrid FSO/RF is implemented and for second phase of communication only FSO is implemented because of negligible atmospheric affects on R-D link [17].

3.2   Organisation of Chapter

The rest of the chapter is organized as follows: The system model for DH hyrbid FSO/RF system has been discussed in Section 3.3. Section 3.4 provides the closed-form expressions for the outage probability and average SER. Furthermore, numerical results and inferences are given in Section 3.5. Finally, the concluding remarks are given in Section 3.6.

3.3 System Model

Let us consider an uplink model as shown in Figure 3.1, where a ground station (S) intends to transmit the signal to satellite S with the help of a single DF relay, which is selected out of N number of relays based on PRS scheme. Here out of N relays, one relay is selected based on the instantaneous SNR between $S \rightarrow R_n$ links, where, $n = 1, 2, ...N$. Here the data transmission takes place in two phases and we assume symbol by symbol transmission. Let $h_{i,j}$ represents the independent Malaga fading channel coefficient between nodes i and j, where $i \neq j$, $i \in \{S, R_n\}$, $j \in \{R_n, D\}$. At the beginning of the transmission, the source node selects one relay based on the CSI.
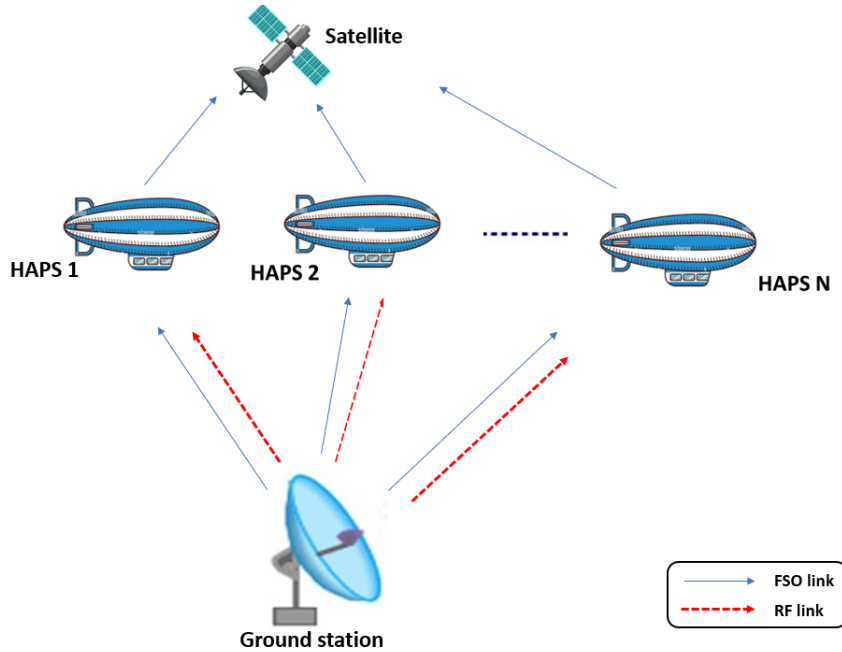
Figure 3.1: System Model

Two-phase orthogonal transmission is used in the suggested system model. During the first phase of the uplink scenario, S transmits the information signal to R across the hybrid FSO/RF link. R delivers the decoded information signal to D over the FSO link during the second or orthogonal phase transmission. One relay is chosen on the value of the instantaneous SNR of S-R FSO links. If the instantaneous SNR of the selected relay is less than the threshold SNR γ_{th}, then the RF link will be activated using a 1-bit feedback signal [16].

First Phase:

The received signals at HAPS relay $R_1, R_2 ... R_n$ are given by

$$y_1 = h_{SR_1} x_1 + n_1 \tag{3.1}$$

$$y_2 = h_{SR_2} x_1 + n_1 \tag{3.2}$$

$$.$$

$$.$$

$$.$$

$$y_n = h_{SR_n} x_1 + n_1 \tag{3.3}$$

where n_1 denote the (AWGN) with zero mean and variance σ^2, h_{SR_1}, $h_{SR_2} ... h_{SR_n}$ are the fading channel coefficients for source to relay link.

Second phase:

The received signal at D in the second phase can be expressed as

$$y_D = h_{R_n D} x_2 + n_2 \tag{3.4}$$

where n_2 represent the AWGN at D with zero mean and variance σ^2, and h_{RD} is the fading channel coefficient for relay to destination link and n value can be any value from 1 to n depending upon which relay is selected.

3.3.1 RF Channel model

Our RF channel is modelled using shadowed kappa-mu $(\kappa - \mu)$ distribution. This distribution mainly based on parameters κ, μ, m where ratio between dominant components and scattered waves, μ denotes the fluctuation level due to shadowing in the dominant component and m is the number of clusters, which is a non-negative real number resulting in a more general and flexible distribution. It is to be noted that large value of κ implies more power in the dominant component with respect to scattered waves and large value of m implies that the dominant component is quite stable due to less shadowing [15]. The PDF of instantaneous SNR of RF link undergoing shadowed $\kappa - \mu$ is given by

$$f_{\gamma^{rf}}(\gamma) = \sum_{q=0}^{\infty} R_{1,q} \gamma^{q+\mu-1} e^{-\mu(1+\kappa)\gamma/\gamma_{avg}} \tag{3.5}$$

where $R_{1,q} = \frac{\mu^{2q+\mu}(1+k)^{\mu+q}}{(\mu k+m)^{m+q}\gamma_{avg}^{\mu+q}}$.

The CDF is obtained from integrating PDF over limits 0 and γ, which is given by

$$F_{\gamma^f}(\gamma) = \int_0^\gamma f_{\gamma^{rf}}(t)\,dt \tag{3.6}$$

By substituting (3.30) in (3.31) $F_{\gamma^f}(\gamma)$ is given by

$$F_{\gamma^f}(\gamma) = \int_0^\gamma \sum_{q=0}^\infty R_{1,q}\gamma^{q+\mu-1}exp(-\mu(1+\kappa)\gamma/\gamma_{avg})\,dt \tag{3.7}$$

Also we have the formula from [7], which is given by

$$\int_0^u x^{v-1}e^{-bx}\,dx = b^{-v}\gamma(v,bu) \tag{3.8}$$

By comparing the equations (3.8) and (3.9), the final expression for CDF will be

$$F_{\gamma^{rf}}(\gamma_{th}) = \sum_{q=0}^\infty R_{1,q}\left[\frac{\mu(1+k)}{\gamma_{avg}}\right]^{-(\mu+q)}\gamma\left(\mu+q,\frac{\mu(1+k)\gamma_{th}}{\gamma_{avg}}\right) \tag{3.9}$$

3.4 Performance Analysis

3.4.1 Outage probability analysis of RF link

The outage probability of the RF link is given by

$$P_{rf}^{out} = P(\gamma < \gamma_{th}) \tag{3.10}$$

where γ_{th} is SNR threshold and expression for outage probability is obtained at γ_{th} in CDF and it is given by

$$P_{rf}^{out} = \sum_{q=0}^\infty R_{1,q}\left[\frac{\mu(1+k)}{\gamma^{rf}}\right]^{-(\mu+q)}\gamma\left(\mu+q,\frac{\mu(1+k)\gamma_{th}}{\gamma_{avg}}\right) \tag{3.11}$$

3.4.2 Outage probability analysis of hybrid FSO/RF link with one HAPS

The outage probability of DH hybrid link is given by

$$P_0^{DH} = 1 - \{(1-P_0^{SR})(1-P_0^{RD})\} \tag{3.12}$$

$$= P_0^{SR} + P_0^{RD} - P_0^{SR}P_0^{RD} \tag{3.13}$$

24

where $P_0^{SR} = F_{\gamma_{SR}^f}(\gamma_{SR}) F_{\gamma_{SR}^{rf}}(\gamma_{SR})$ and $P_0^{RD} = F_{\gamma_{RD}^f}(\gamma_{RD})$. Note that $F_{\gamma_{SR}^f}(\gamma_{SR})$ is given by (2.13) and $F_{\gamma_{SR}^{rf}}(\gamma_{SR})$ is taken from (3.11)

$$F_{\gamma_{SR}^f}(\gamma_{SR}) = D_1 \sum_{m=1}^{\beta} c_m G_{r+1,3r+1}^{3r,1} \left(\frac{E\gamma_{SR}}{\gamma} \middle| \begin{matrix} 1,k_1 \\ k_2,0 \end{matrix} \right) \tag{3.14}$$

$$F_{\gamma_{SR}^{rf}}(\gamma_{SR}) = \sum_{q=0}^{\infty} R_{1,q} \left[\frac{\mu(1+k)}{\gamma_{avg}} \right]^{-(\mu+q)} \gamma\left(\mu+q, \frac{\mu(1+k)\gamma_{SR}}{\gamma_{avg}} \right) \tag{3.15}$$

P_0^{RD} is negligible (almost zero) due to negligible atmospheric affects in relay to destination region. The final expression for DH outage probability with single HAPS is majorly dependent on S-R link outage probability i.e. the product of (3.14) and (3.15).

3.4.3   Outage probability analysis of hybrid FSO/RF link with multiple HAPS

The outage probability of DH link with multiple HAPS is obtained when SR_1, SR_2, ...SR_n links are in outage along with the RD link and it is mathematically represented as

$$P_1^{DH} = P\left(max(\gamma_{SR_1}, \gamma_{SR_2}....\gamma_{SR_n}) < \gamma_{th} \cap \gamma_{RD} < \gamma_{th} \right) \tag{3.16}$$

This can also be written as

$$P_1^{DH} = 1 - \{(1-P_1^{SR})(1-P_1^{RD})\} \tag{3.17}$$

$$= P_1^{SR} + P_1^{RD} - P_1^{SR}P_1^{RD} \tag{3.18}$$

where $P_1^{SR} = [F_{\gamma_{SR_1}^f}(\gamma_{SR_1}) F_{\gamma_{SR_2}^f}(\gamma_{SR_2})..F_{\gamma_{SR_n}^f}(\gamma_{SR_n})] \times F_{\gamma_{SR}^{rf}}(\gamma_{SR})$ and $P_1^{RD} = F_{\gamma_{RD}^f}(\gamma_{RD})$. By substituting the corresponding expressions, the final expression for P_1^{SR} is obtained as (we have assumed that all links are identical)

$$P_1^{SR} = \left[D_1 \sum_{m=1}^{\beta} c_m G_{r+1,3r+1}^{3r,1} \left(\frac{E\gamma_{SR}}{\gamma_{avg}} \middle| \begin{matrix} 1,k_1 \\ k_2,0 \end{matrix} \right) \right]^N$$
$$\times \sum_{q=0}^{\infty} R_{1,q} \left[\frac{\mu(1+k)}{\gamma_{avg}} \right]^{-(\mu+q)} \gamma\left(\mu+q, \frac{\mu(1+k)\gamma_{SR}}{\gamma_{avg}} \right) \tag{3.19}$$

P_1^{RD} is almost negligible (almost zero). The final expression for DH outage probability with multiple HAPS is majorly dependent on S-R link outage probability. After substituting P_1^{SR}

and P_1^{RD} values in (3.18). The final expression will be

$$P_1^{DH} = \left[D_1 \sum_{m=1}^{\beta} c_m G_{r+1,3r+1}^{3r,1} \left(\frac{E\gamma_{SR}}{\gamma_{avg}} \middle| \begin{matrix} 1,k_1 \\ k_2,0 \end{matrix} \right) \right]^N$$

$$\times \sum_{q=0}^{\infty} R_{1,q} \left[\frac{\mu(1+k)}{\gamma_{avg}} \right]^{-(\mu+q)} \gamma\left(\mu+q, \frac{\mu(1+k)\gamma_{SR}}{\gamma_{avg}} \right) \tag{3.20}$$

3.4.4 Symbol error rate of a RF link

The average SER of RF link is obtained by integrating the product of conditional SER and instantaneous SNR of RF link, which is given by

$$P_e^{rf} = \int_0^{\infty} p(e/\gamma_{ii}) f_{\gamma_{ii}^{rf}}(\gamma_{ii}) d\gamma_{ii} \tag{3.21}$$

After substituting the corresponding terms in (3.21), the average SER is given by

$$P_e^{rf} = \int_0^{\infty} \frac{A}{2\sqrt{\pi}} G_{1,2}^{2,0}\left(B^2\gamma \middle| \begin{matrix} 1 \\ \alpha,\beta \end{matrix} \right) \sum_{q=0}^{\infty} R_{1,q} \gamma^{q+\mu-1} e^{-\mu(1+\kappa)\gamma/\gamma_{avg}} d\gamma \tag{3.22}$$

Using [11, eq.7.34.21.0088.01] and simplifying above integral gives average SER of RF link and it is given by

$$P_e^{rf} = \sum_{q=0}^{\infty} R_{1,q} \left[\frac{\mu(1+k)}{\gamma_{avg}} \right]^{-\mu+q} G_{2,2}^{2,1}\left(\frac{B^2\gamma_{avg}}{\mu(1+\kappa)} \middle| \begin{matrix} 1-q-\mu,1 \\ 0,0.5,- \end{matrix} \right) \tag{3.23}$$

3.4.5 Average SER of uplink hybrid FSO/RF with single HAPS

The conditional SER of S-R-D link during uplink can be written as

$$P_{e_{SRD}}(\gamma_{SR},\gamma_{RD}) = P_e(\gamma_{SR}) + P_e(\gamma_{RD}) - P_e(\gamma_{SR}) P_e(\gamma_{RD}). \tag{3.24}$$

After averaging (3.24) over the PDFs of the instantaneous SNR values of FSO link, the average SER is given by

$$P_e^{SRD} = P_e^{SR} + P_e^{RD} - P_e^{SR} P_e^{RD} \tag{3.25}$$

where $P_e^{SR} = P_{SR}^f(\gamma_{th}) + F_{\gamma_{SR}}(\gamma_{th}) P_{SR}^{rf}$ and here, $P_{SR}^f(\gamma_{th})$ represents average SER of FSO link during non outage period, P_{SR}^{rf} represents average SER of RF link and $F_{\gamma_{SR}}(\gamma_{th})$ represents outage probability of FSO link. Note that $F_{\gamma_{SR}}(\gamma_{th})$ and $P_{SR}^f(\gamma_{th})$ are, respectively, given by

$$F_{\gamma_{SR}}(\gamma_{th}) = D_1 \sum_{m=1}^{\beta} c_m G_{r+1,3r+1}^{3r,1}\left(\frac{E\gamma_{th}}{\gamma_{avg}} \middle| \begin{matrix} 1,k_1 \\ k_2,0 \end{matrix} \right) \tag{3.26}$$

$$P_{SR}^{rf} = \sum_{q=0}^{\infty} R_{1,q} \left[\frac{\mu(1+k)}{\gamma_{avg}}\right]^{-\mu+q} G_{2,2}^{2,1} \left(\frac{B^2 \gamma_{avg}}{\mu(1+\kappa)} \middle| \begin{matrix} 1-q-\mu, 1 \\ 0, 0.5, - \end{matrix}\right) \tag{3.27}$$

$P_{SR}^{f}(\gamma_{th})$ can be obtained by solving below integral

$$P_{SR}^{f}(\gamma_{th}) = \int_{\gamma_{th}}^{\infty} p(e/\gamma_{ii}) f_{\gamma_{ii}^f}(\gamma_{ii}) \, d\gamma_{ii} \tag{3.28}$$

$$P_{SR}^{f}(\gamma_{th}) = \int_{0}^{\infty} p(e/\gamma_{ii}) f_{\gamma_{ii}^f}(\gamma_{ii}) \, d\gamma_{ii} - \underbrace{\int_{0}^{\gamma_{th}} p(e/\gamma_{ii}) f_{\gamma_{ii}^f}(\gamma_{ii}) \, d\gamma_{ii}}_{I} \tag{3.29}$$

First integral term has already been derived and it was given in (2.27), whereas second integral term is given by

$$I = \int_{0}^{\gamma_{th}} \frac{A}{2\sqrt{\pi}} G_{1,2}^{2,0} \left(B^2 \gamma_{ii} \middle| \begin{matrix} 1 \\ \alpha, \beta \end{matrix}\right) D_1 \sum_{m=1}^{\beta} \frac{b_m}{\gamma_{ii}} G_{1,3}^{3,0} \left(B_1 \left(\frac{\gamma_{ii}}{\gamma_{avg}}\right)^{\frac{1}{r}} \middle| \begin{matrix} g^2+1 \\ g^2, \alpha_{ii}, m_{ii} \end{matrix}\right) d\gamma_{ii} \tag{3.30}$$

Simplifying the equation by writing Meijer-G function in summation series, we get

$$I = \int_{0}^{\gamma_{th}} \frac{A}{2} \left\{1 - \frac{2}{\sqrt{\pi}} \sum_{k=0}^{\infty} \frac{(-1)^k (\gamma_{ii})^{\frac{2k+1}{2}} B^{2k+1}}{k!(2k+1)}\right\} D_1$$
$$\times \sum_{m=1}^{\beta} \frac{b_m}{\gamma_{ii}} G_{1,3}^{3,0} \left(B_1 \left(\frac{\gamma_{ii}}{\gamma_{avg}}\right)^{\frac{1}{r}} \middle| \begin{matrix} g^2+1 \\ g^2, \alpha_{ii}, m_{ii} \end{matrix}\right) d\gamma_{ii} \tag{3.31}$$

After separating above expression into two integral terms, we obtain

$$I = \underbrace{\int_{0}^{\gamma_{th}} \frac{AD_1}{2} \sum_{m=1}^{\beta} \frac{b_m}{\gamma_{ii}} G_{1,3}^{3,0} \left(B_1 \left(\frac{\gamma_{ii}}{\gamma_{avg}}\right)^{\frac{1}{r}} \middle| \begin{matrix} g^2+1 \\ g^2, \alpha_{ii}, m_{ii} \end{matrix}\right) d\gamma_{ii}}_{I_1}$$
$$- \underbrace{\int_{0}^{\gamma_{th}} \frac{2}{\sqrt{\pi}} \sum_{k=0}^{\infty} \frac{(-1)^k (\gamma_{ii})^{\frac{2k+1}{2}} B^{2k+1}}{k!(2k+1)} D_1 \sum_{m=1}^{\beta} \frac{b_m}{\gamma_{ii}} G_{1,3}^{3,0} \left(B_1 \left(\frac{\gamma_{ii}}{\gamma_{avg}}\right)^{\frac{1}{r}} \middle| \begin{matrix} g^2+1 \\ g^2, \alpha_{ii}, m_{ii} \end{matrix}\right) d\gamma_{ii}}_{I_2}$$
$$\tag{3.32}$$

Here I_1 is the CDF of FSO link and I_2 is simplified using [11, eq.7.34.21.0084.01] and it is given by

$$I_2 = C_2 \sum_{m=1}^{\beta} C_m \sum_{n=0}^{\infty} D_n G_{r+1,3r+1}^{3r,1} \left(E \left(\frac{\gamma_{ii}}{\gamma}\right) \middle| \begin{matrix} -n+0.5, k_1 \\ k_2, -n-0.5 \end{matrix}\right) \tag{3.33}$$

where $C_2 = \frac{AA^1 \rho^2}{2^{2r} \pi^{r-0.5}}$ and $D_n = \frac{2(-1)^n B^{2n+1} \gamma_{th}^{n+0.5}}{n!(2n+1)!}$. For R-D part, the link acts as AWGN channel and hence, the average SER is given by

$$p_e^{RD} = \frac{A}{2} \text{erfc} \left(\sqrt{\gamma_{avg}} B\right) \tag{3.34}$$

27

3.4.6 Average SER of uplink hybrid FSO/RF with multiple HAPS

While calculating average SER for multiple HAPS scenario, the only thing that changes from single HAPS scenario is S-R part, which is given by

$$P_e^{SR} = P_{SR}^f(\gamma_{th}) + F_{\gamma_{SR}}(\gamma_{th}) P_{SR}^{rf} \tag{3.35}$$

where $P_{SR}^{rf} = \sum_{q=0}^{\infty} R_{1,q} \left[\frac{\mu(1+k)}{\gamma_{avg}} \right]^{-\mu+q} G_{2,2}^{2,1} \left(\frac{B^2 \gamma_{avg}}{\mu(1+\kappa)} \middle| \begin{array}{c} 1-q-\mu,1 \\ 0,0.5,- \end{array} \right) \tag{3.36}$

In the case of hybrid link with multiple HAPS, gamma-gamma distribution has been considered for the FSO channel modelling [4] and in particular, for calculation of average SER [3]. In this case, the PDF of instantaneous SNR of FSO link is given by

$$f_{\gamma_{ii}}(\gamma_{ii}) = \frac{g^2}{2\Gamma(\alpha)\Gamma(\beta)\gamma_{ii}} G_{1,3}^{3,0} \left(\alpha\beta k \left(\frac{\gamma_{ii}}{\gamma_{avg}} \right)^{\frac{1}{2}} \middle| \begin{array}{c} g^2+1 \\ g^2,\alpha,\beta \end{array} \right) \tag{3.37}$$

The CDF is given by

$$F_{\gamma_{ii}}(\gamma_{ii}) = \frac{g^2}{\Gamma(\alpha)\Gamma(\beta)\gamma_{ii}} G_{2,4}^{3,1} \left(\alpha\beta k \left(\frac{\gamma_{ii}}{\gamma_{avg}} \right)^{\frac{1}{2}} \middle| \begin{array}{c} 1,g^2+1 \\ g^2,\alpha,\beta \end{array} \right) \tag{3.38}$$

While calculating average SER in order to solve the integral, we have to modify the CDF expression. It can also be written as

$$F_{\gamma_{ii}}(\gamma_{ii}) = \frac{g^2}{\Gamma(\alpha)\Gamma(\beta)} \sum_{p=1}^{\beta} X_p \tag{3.39}$$

where $X_1 = z^{g^2} C_1 \sum_{t=0}^{\infty} \frac{\Gamma(g^2+t)z^t}{\Gamma(t+g^2-\alpha+1)\Gamma(t+g^2-\beta+1)\Gamma(t+g^2+1)\Gamma(g^2)}$

$X_2 = z^{\alpha} C_2 \sum_{t=0}^{\infty} \frac{\Gamma(\alpha+t)\Gamma(t-g^2+\alpha)z^t}{\Gamma(t-g^2+\alpha+1)\Gamma(t+\alpha-\beta+1)\Gamma(t+\alpha+1)\Gamma(\alpha)\Gamma(\alpha-g^2)}$

$X_3 = z^{\beta} C_3 \sum_{t=0}^{\infty} \frac{\Gamma(\beta+t)\Gamma(t-g^2+\beta)z^t}{\Gamma(t-g^2+\beta+1)\Gamma(t-\alpha+\beta+1)\Gamma(t+\beta+1)\Gamma(\beta)\Gamma(\beta-g^2)}$

and $z = \frac{\alpha\beta k \gamma_{ii}^{1/2}}{\gamma^{1/2}}$

$C_1 = \frac{\csc(\pi(\alpha-\rho^2))\csc(\pi(\beta-\rho^2))}{1}$, $C_2 = \frac{\csc(\pi(\rho^2-\alpha))\csc(\pi(\beta-\alpha))}{(\rho^2+1-\alpha)}$, $C_3 = \frac{\csc(\pi(\rho^2-\beta))\csc(\pi(\alpha-\beta))}{(\rho^2+1-\beta)}$

The PDF of FSO link in the case of multiple HAPS is given by

$$f_\gamma(\gamma) = N \times f_{\gamma_{SR}}(\gamma_{SR})[F_{\gamma_{SR}}(\gamma_{SR})]^{N-1} \tag{3.40}$$

The Average SER of FSO link in the case of multiple HAPS is given by

$$P_{SR}^f(\gamma_{th}) = \int_{\gamma_{th}}^{\infty} P(e/\gamma_{SR}) f_{\gamma_{SR}}(\gamma_{SR})[F_{\gamma_{SR}}(\gamma_{SR})]^{N-1} \, d\gamma_{SR} \tag{3.41}$$

Because of the constraints in the calculation of average SER of generalized N links case, we are considering the special case of $N = 2$ and the average SER is given by

$$P_{SR}^{f}(\gamma_{th}) = 2 \times \int_{\gamma_{th}}^{\infty} P(e/\gamma_{SR}) f_{\gamma_{SR}}(\gamma_{SR}) F_{\gamma_{SR}}(\gamma_{SR}) \, d\gamma_{SR} \tag{3.42}$$

$$= \underbrace{\int_{0}^{\infty} 2P(e/\gamma_{SR}) f_{\gamma_{SR}}(\gamma_{SR}) F_{\gamma_{SR}}(\gamma_{SR}) \, d\gamma_{SR}}_{I} - \underbrace{\int_{0}^{\gamma_{th}} 2P(e/\gamma_{SR}) f_{\gamma_{SR}}(\gamma_{SR}) F_{\gamma_{SR}}(\gamma_{SR}) \, d\gamma_{SR}}_{J} \tag{3.43}$$

I in (3.43) can be simplified by substituting corresponding expressions and using [11, eq.7.34.21.0013.01]

$$I = C_0 \left[\frac{\rho^2}{\Gamma(\alpha)\Gamma(\beta)} \right]^2 \frac{2^{\alpha+\beta-1}}{2\pi} B^{\rho^2+k} G_{4,7}^{6,2} \left(\frac{(\alpha\beta k)^2}{16B^2 \gamma_{avg}} \middle| \begin{array}{l} 1-\tau, 0.5-\tau, \kappa_1 \\ \\ \kappa_2, -\tau \end{array} \right) \tag{3.44}$$

J in (3.43) can be simplified by substituting corresponding expressions and using [11, eq.7.34.21.0084.01]

$$J = \frac{AC_0}{2} \left[\frac{\rho^2}{\Gamma(\alpha)\Gamma(\beta)} \right]^2 \frac{2^{\alpha+\beta-1}}{2\pi\gamma_{th}^{-\tau}} G_{3,7}^{6,1} \left(\frac{(\alpha\beta k)^2 \gamma_{th}}{16\gamma_{avg}} \middle| \begin{array}{l} 1-\tau, \kappa_1 \\ \\ \kappa_2, -\tau \end{array} \right)$$

$$- \frac{AC_0}{2\sqrt{\pi}} \sum_{k_n=0}^{\infty} \frac{(-1)_n^k B^{2k_n+1}}{k_n!(2k_n+1)} \frac{2^{\alpha+\beta-1}}{2\pi\gamma_{th}^{-\tau}} G_{3,7}^{6,1} \left(\frac{(\alpha\beta k)^2 \gamma_{th}}{16\gamma_{avg}} \middle| \begin{array}{l} 1-\tau_1, \kappa_1 \\ \\ \kappa_2, -\tau_1 \end{array} \right) \tag{3.45}$$

where $\tau_1 = \frac{2k_n+1}{2} + \frac{\rho^2+k}{2} - 1$, $\tau = \frac{\rho^2+k}{2}$, $C_0 = \sum_{p=1}^{3} \frac{X_p}{w_p}$ and $w_1 = \gamma^{g^2+k}$, $w_2 = \gamma^{\alpha+k}$, $w_3 = \gamma^{\beta+k}$

Finally, by substituting these obtained expressions in (3.35), P_e^{SR} is obtained. For R-D link scenario, the link acts as AWGN channel and hence, the average SER is given by

$$p_e^{RD} = \frac{A}{2} \text{erfc} \left(\sqrt{\gamma_{avg}} B \right) \tag{3.46}$$

3.5 Numerical Results and Discussions

In this section, we will analyze the derived closed-form expressions. We also demonstrate the effects of various parameters on outage probability (OP) and average SER for the proposed system model. For numerical investigation, we set threshold SNR $\gamma_{th} = 5$ dB, height at which HAPS is located at 20km, $\lambda = 1.55\mu m$, $\alpha_{SR} = 2.89, \beta_{SR} = 2, \alpha_{RD} = 801.6, \beta_{RD} = 1024$ and parameters considered for making conclusions are pointing error coefficient, wind velocity and zenith angle.
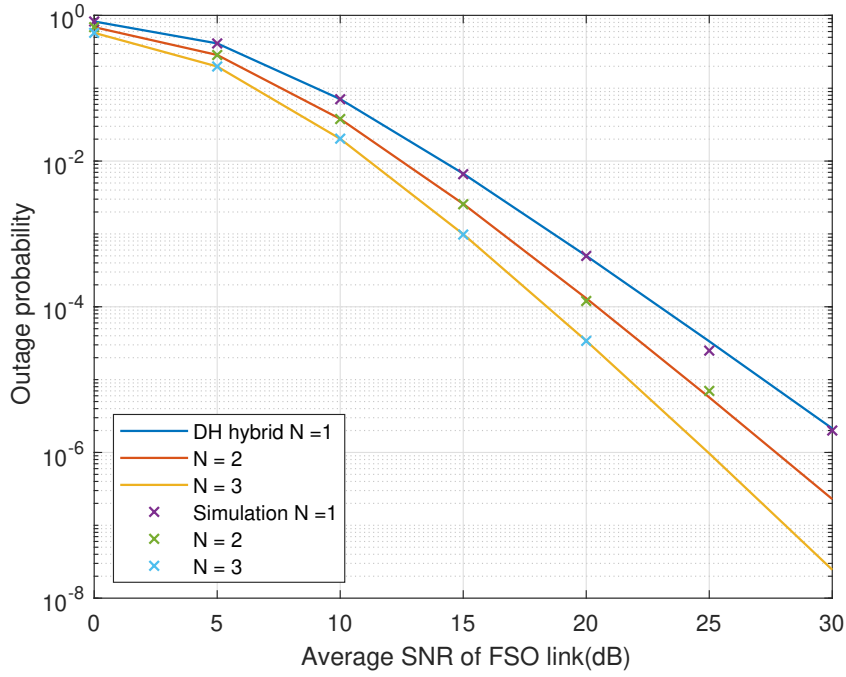
Figure 3.2: OP vs Avg. SNR of FSO link for different values of N

Figure 3.2 shows the effect of number of relays in system (N) on the outage probability. From the plot, we can observe that outage performance improves with the increase in value of N. Because if more relays are employed in this system, then the best relay can be selected out of N relays. The SNRs required for the system to achieve the outage probability of 10^{-2}, with $N=1$, $N=2$, and $N=3$ are 14 dB, 13 dB, 11 dB, respectively. So, the SNR gains achieved by the system with $N=2$, $N=3$ w.r.t system with $N=1$ are 1 dB, 2 dB, respectively. From this we can conclude that with the increase in value of N, and there isn't much improvement in the SNR gain. The outage probability tends to decrease, when SNR increases. Because as SNR increases, the signal becomes much stronger than the noise.
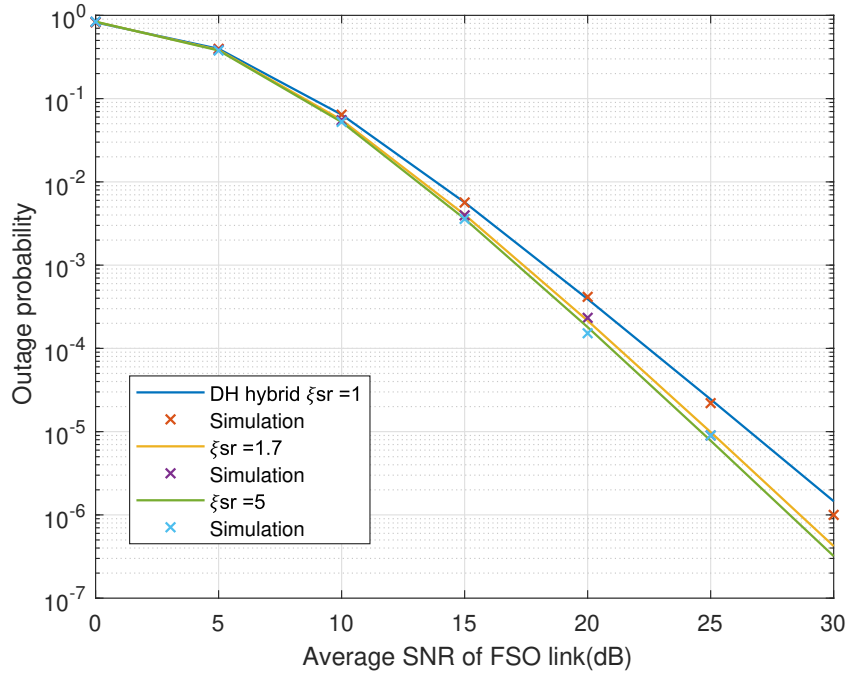
Figure 3.3: OP vs Avg. SNR of FSO link for different values of ξ_{sr}

Figure 3.3 shows the effect of value of pointing error coefficient ζ_{SR} on the outage probability. From the plot, we can observe that the outage performance improves with the increase in ζ_{SR}. Because, increase in pointing error coefficient implies decrease in pointing errors. To achieve the outage probability of 10^{-2}, the SNRs required for the system with $\zeta_{SR}=1$, $\zeta_{SR}=1.7$, $\zeta_{SR}=5$, are 14 dB, 13 dB, 8 dB, 12.5 dB, respectively. Thus, the SNR gains achieved by the system with $\zeta_{SR}=1$ w.r.t system with $\zeta_{SR}=1.7$, $\zeta_{SR}=5$ are 1 dB, 0.5 dB respectively. We can conclude that with the increase in value of ζ_{SR}, there is not much improvement in SNR gain.

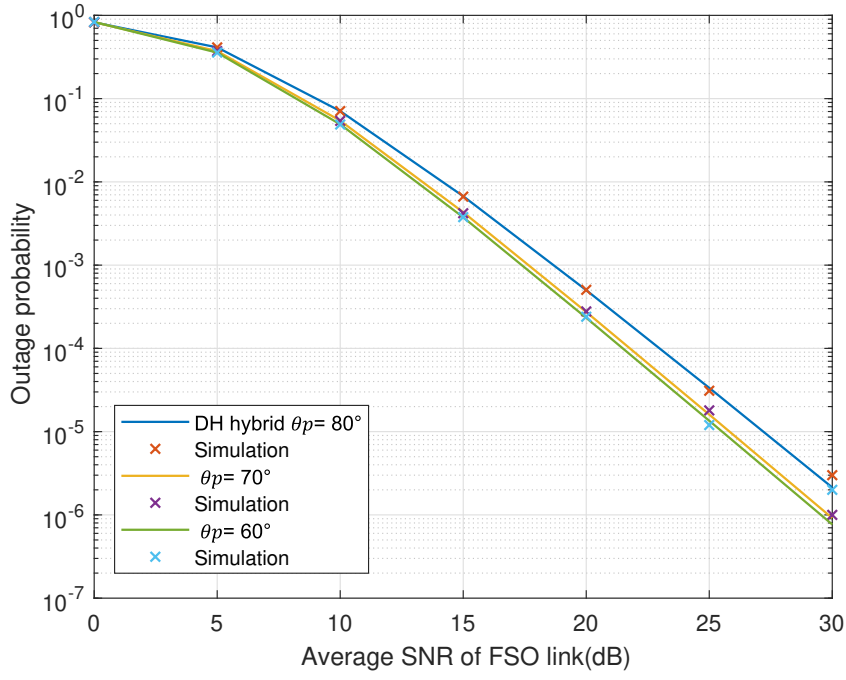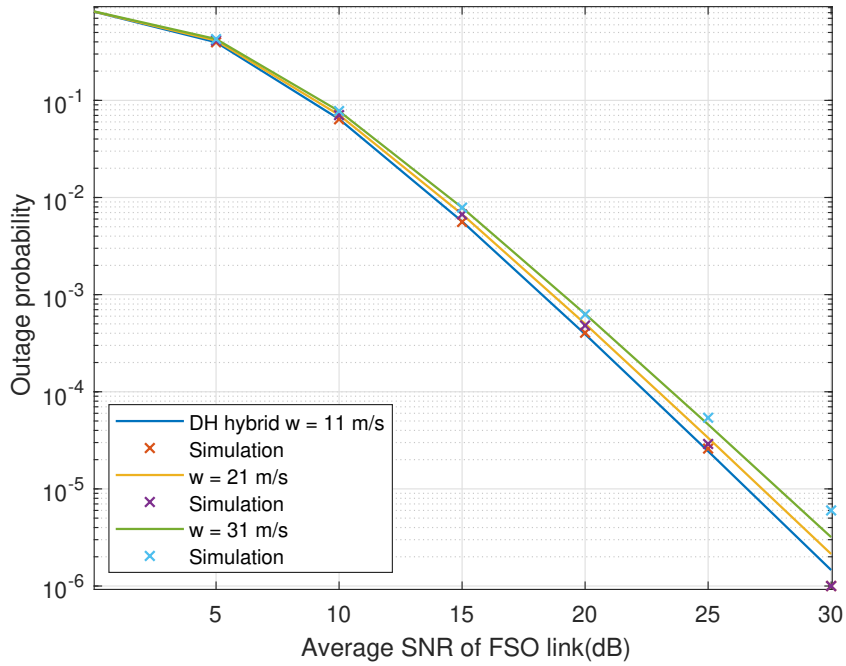Figure 3.4: OP vs. Avg. SNR of FSO link for different values of θ_p

Figure 3.5: OP vs. Avg. SNR of FSO link for different values of w

Figure 3.4 and 3.5 show the effect of the wind velocity and zenith angle on system model w.r.t to outage probability. From both figures, we can observe that outage performance decreases with the increase in value of w and θ_p. The reason in case of wind velocity is

that as wind velocity increases the disturbance in atmosphere increases and thus, the link performance degrades. While in the case of zenith angle, it is directly proportional to link distance i.e. greater the zenith angle, greater the link distance and hence, probability for system in outage increases.

Figure 3.6: SER vs. Avg. SNR of FSO link for different system models
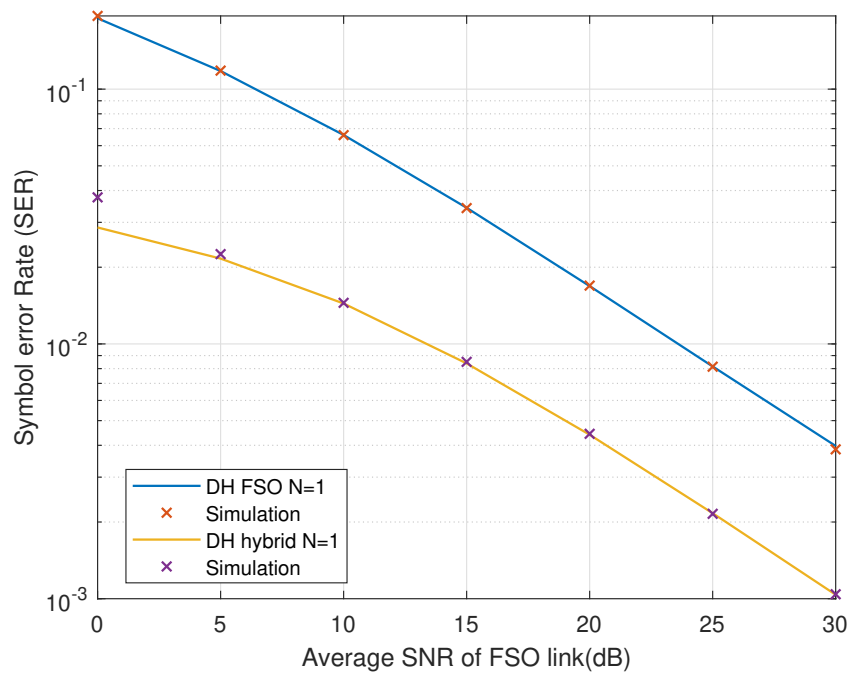
Figure 3.6 shows the comparison between two system models i.e. DH FSO and DH hybrid on the basis of average SER. We can clearly see that to achieve SER of 10^{-2}, hybrid system requires average SNR of 14 dB and FSO system requires 24 dB. The SNR gain is 10 dB. Thus, we can conclude that hybrid system has better average SER performance compared to FSO system .
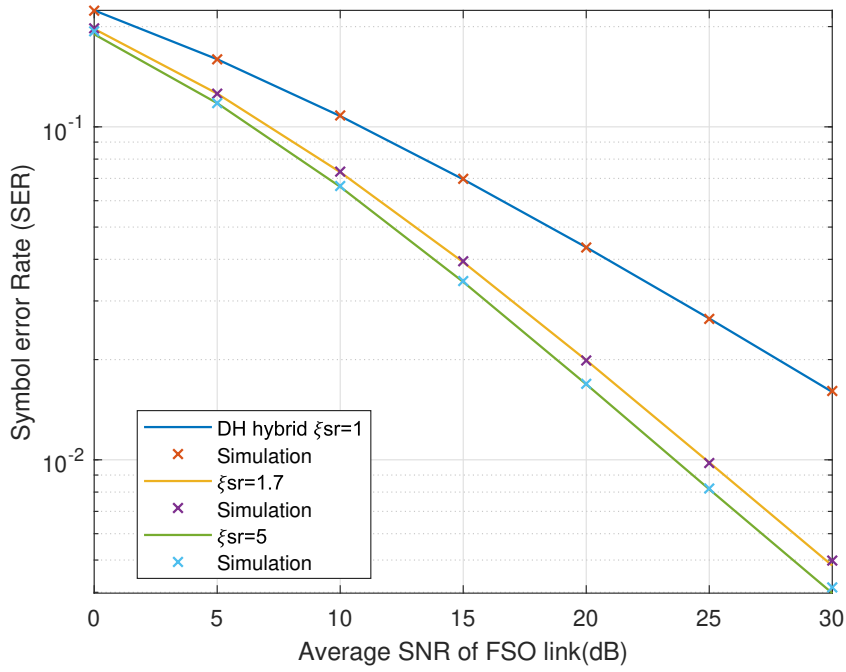
Figure 3.7: SER vs Avg. SNR of FSO link for different values of ζ_{SR}

Figure 3.7 shows the effect of value of pointing error coefficient ζ_{SR} on the average SER. From the plot, we can observe that with the increase in ζ_{SR}, the SER performance improves. Because, increase in pointing error coefficient implies decrease in pointing errors. The SNRs required to achieve the SER of 10^{-1} for the system with $\zeta_{SR}=1$, $\zeta_{SR}=1.7$, $\zeta_{SR}=5$ are 11 dB, 7 dB, and 6.5 dB respectively. So, the SNR gains achieved by the system with $\zeta_{SR}=1$ w.r.t system with $\zeta_{SR}=1.7$, $\zeta_{SR}=5$ are 4 dB and 4.5 dB, respectively. We can conclude that with the increase in value of ζ_{SR} above 1.7, there is not much improvement in SNR gain.

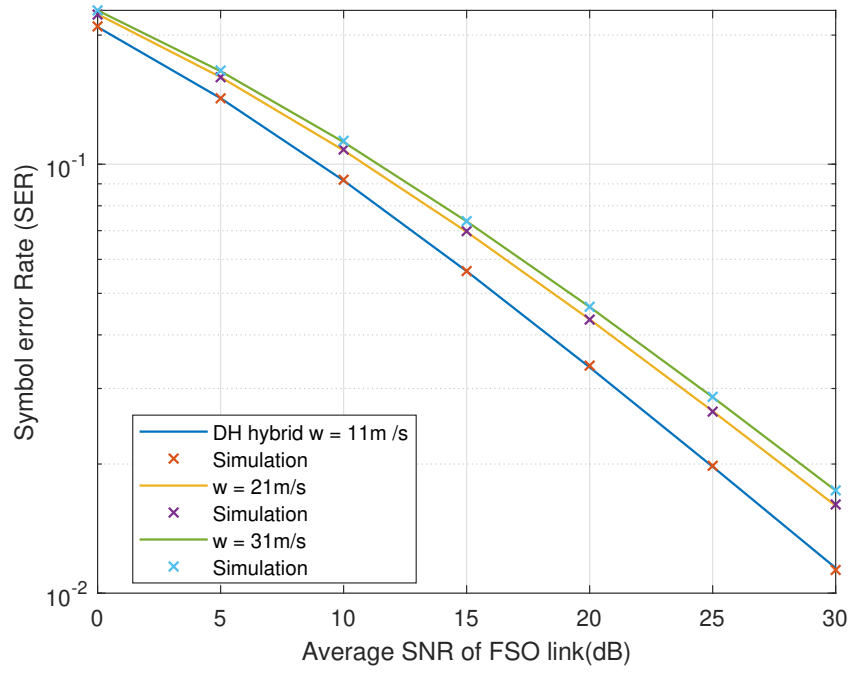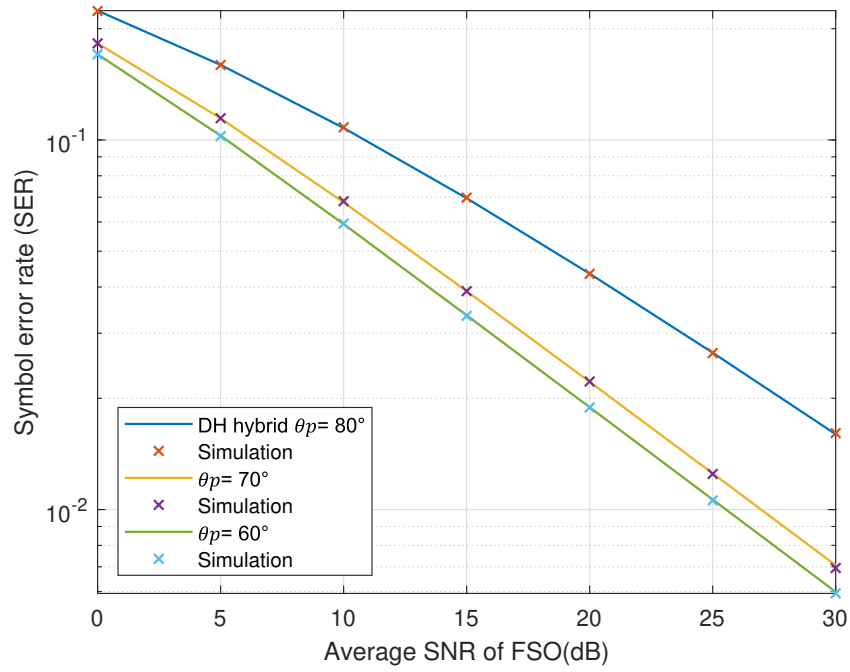Figure 3.8: SER vs. Avg SNR of FSO link for different values of w

Figure 3.9: SER vs. Average SNR of FSO link for different values of θ_p

Figure 3.8 and 3.9 shows effect of the wind velocity and zenith angle on average SER. From both figures, we can observe that SER performance decreases with increase in value of w and θ_p due to the reasons which are mentioned previously.

3.6 Conclusions

The performance of the DH hybrid FSO/RF system model is examined in this chapter by deriving outage probability and average SER expressions in closed-form over Malaga and shadowed $\kappa - \mu$ fading channels. In addition, MATLAB is used to compute the closed-form expressions. The outage performance of the proposed system model improves as the value of N increases and the outage performance of the system with relay is better than the system without relay. Furthermore, it has been discovered that the DH hybrid system outperforms the DH FSO system. Finally, the theoretical outage probability and SER values accord well with the simulated outage probability and SER values acquired from Monte Carlo simulations, which validate the derived expressions.

Chapter 4

End-to-End Performance Analysis of multiple HAPS-based Hybrid FSO/RF Communication

4.1 Introduction

The exact expressions for DH hybrid FSO/RF system model are derived over Malaga fading channels in Chapter 3. The proposed system model in Chapter 3 has achieved good performance for uplink communication. Now we work on performance analysis of end-to-end system considering both uplink and downlink scenarios. This system model consists of ground station, uplink and downlink HAPS-based relays, and satellite. In the first phase of downlink communication i.e. from satellite to relay, FSO link is used and in second phase i.e. relay to ground station, RF link is used. The performance of this proposed system is analyzed by deriving the exact outage probability and average SER expressions over Malaga and shadowed $\kappa - \mu$ fading channels.

4.2 Organisation of chapter

The rest of the chapter is organized as follows: The system model for end-to-end communication has been discussed in Section 4.3. Section 4.4 provides the closed-form expressions for outage probability and SER over Malaga fading channels. Furthermore, numerical results and inferences are given in Section 4.5. Finally, the concluding remarks are given in

Section 4.6.

4.3 System Model

In this chapter, end-to-end performance analysis will be done in four stages. In uplink during the first phase of the transmission, S transmits the information signal to R across the hybrid FSO/RF link (Fig.4.1) or FSO link (Fig.4.2). After that R delivers the decoded information signal to D over the FSO link during the second or orthogonal phase transmission. One relay is chosen from two relay nodes based on the value of the instantaneous SNR of S-R links. After that FSO link is used for transmission from HAPS to satellite. For downlink, FSO link is used for transmission from satellite to HAPS and finally, RF link is used for transmission between HAPS and GS [21].

In the first stage, the signal is transmitted from GS to HAPS and then HAPS will decode and forward the received signal to satellite. Further, satellite again decodes and forwards the signal to HAPS and finally, HAPS decodes the signal and transmits to GS [6].
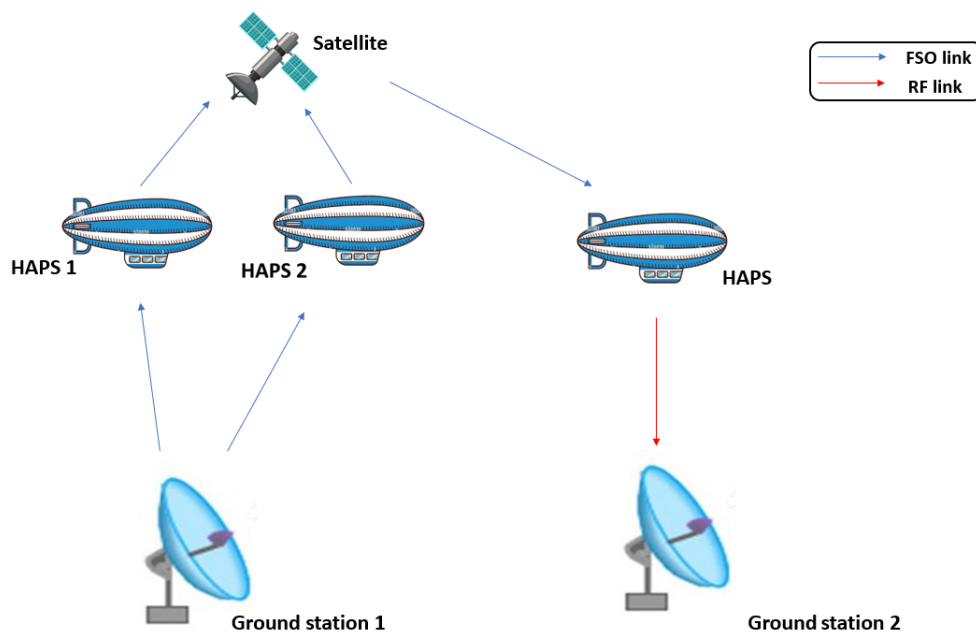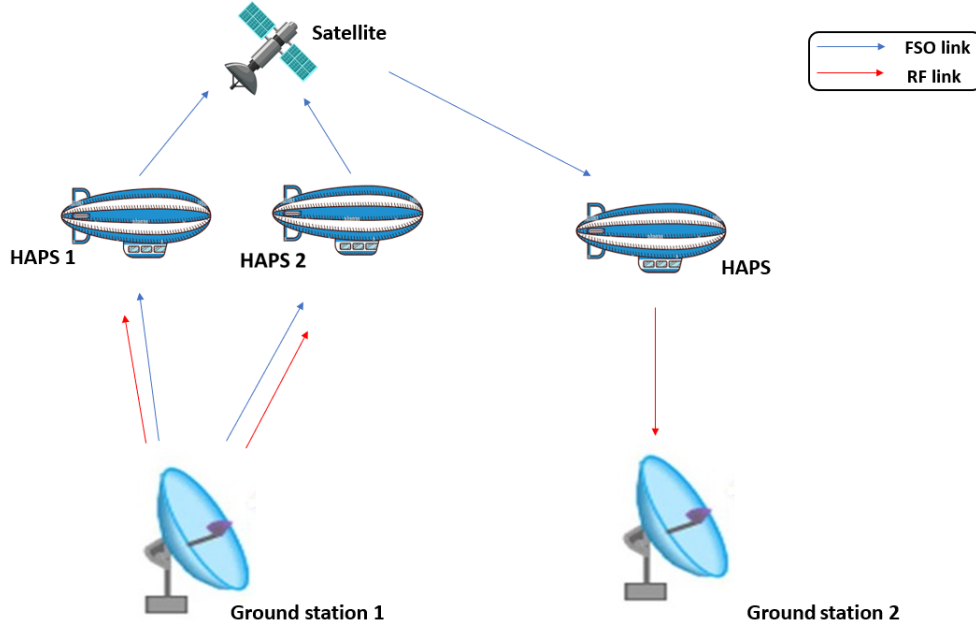

Figure 4.1: System Model I

38

Figure 4.2: System Model II

First Phase: The received signals at HAPS relays R_1, R_2 are given by (assuming two relays)

$$y_1 = h_{SR_1} x_1 + n_1 \qquad (4.1)$$

$$y_2 = h_{SR_2} x_1 + n_1 \qquad (4.2)$$

where n_1 represents the additive white gaussian noise (AWGN) with zero mean and variance σ^2, h_{SR_1} and h_{SR_2} are the fading channel coefficients.

Second phase: The received signal at D in the second phase can be expressed as

$$y_3 = h_{RD} x_2 + n_2 \qquad (4.3)$$

where n_2 represents the AWGN at D with zero-mean and variance σ^2.

Third phase: The received signal at R_1 from satellite S_1 in the third phase can be expressed as

$$y_4 = h_{S_1 R_1} x_3 + n_2 \qquad (4.4)$$

Fourth phase: The received signal at D_1 during the fourth phase can be expressed as

$$y_5 = h_{R_1 D_1} x_4 + n_3 \qquad (4.5)$$

where n_3 represents the AWGN at D_1 with zero mean and variance σ^2.

4.4 Performance Analysis

4.4.1 Outage probability analysis of End-to-End Communication with Single HAPS

The outage probability of the proposed system model is given by

$$P_{out} = P_{UL} + P_{DL} - P_{UL}P_{DL} \tag{4.6}$$

where

$$P_{UL} = P_{SR} + P_{RD} - P_{SR}P_{RD} \tag{4.7}$$

and

$$P_{DL} = P_{S_1R_1} + P_{R_1D_1} - P_{S_1R_1}P_{R_1D_1} \tag{4.8}$$

P_{UL} has already been derived in Chapter 2 i.e. $F_{\gamma_{SR}^f}(\gamma_{SR})$ and now we have to calculate for P_{DL}. $P_{S_1R_1}$ is the outage probability of satellite to HAPS link, for which the outage probability is negligible or almost zero due to negligible atmospheric affects in this link [9]. $P_{R_1D_1}$ is outage probability of HAPS to GS in downlink. In this part, RF link is used for communication. Therefore, outage probability of RF link is given by

$$P_{R_1D_1} = P_{rf}^{out} = \sum_{q=0}^{\infty} R_{1,q} \left[\frac{\mu(1+k)}{\gamma_{avg}} \right]^{-(\mu+q)} \gamma \left(\mu+q, \frac{\mu(1+k)\gamma_{th}}{\gamma_{avg}} \right) \tag{4.9}$$

Finally, $P_{DL} \approx P_{R_1D_1}$, as $P_{S_1R_1} \approx 0$. By substituting corresponding values of P_{UL} and P_{DL} in (4.33), outage probability is obtained.

4.4.2 Outage probability analysis of End-to-End FSO Communication with multiple HAPS

The outage probability of this system model is given by

$$P_{out} = P_{UL} + P_{DL} - P_{UL}P_{DL} \tag{4.10}$$

where

$$P_{UL} = P_{SR} + P_{RD} - P_{SR}P_{RD} \tag{4.11}$$

and

$$P_{DL} = P_{S_1R_1} + P_{R_1D_1} - P_{S_1R_1}P_{R_1D_1} \tag{4.12}$$

P_{UL} has already been derived in Chapter 2 i.e. $[F_{\gamma_{SR}^f}(\gamma_{SR})]^N$. Now we have to calculate for P_{DL}. $P_{S_1R_1}$ is the outage probability of satellite to HAPS link for which outage probability is negligible or almost zero due to negligible atmospheric affects in this region. $P_{R_1D_1}$ is the outage probability of HAPS to GS in downlink. In this region, RF link is used for communication. Therefore, outage probability of RF link is given by

$$P_{R_1D_1} = P_{rf}^{out} = \sum_{q=0}^{\infty} R_{1,q} \left[\frac{\mu(1+k)}{\gamma_{avg}} \right]^{-(\mu+q)} \gamma\left(\mu+q, \frac{\mu(1+k)\gamma_{th}}{\gamma_{avg}} \right) \tag{4.13}$$

Finally, $P_{DL} \approx P_{R_1D_1}$, since $P_{S_1R_1} \approx 0$. By substituting corresponding values of P_{UL} and P_{DL} in (4.10), outage probability is obtained. The only change we can observe here compared to 4.4.1 is P_{UL} part, especially P_{SR}.

4.4.3 Outage analysis of End-to-End Communication using Hybrid Link

The outage probability of this system model is given by

$$P_{out} = P_{UL} + P_{DL} - P_{UL}P_{DL} \tag{4.14}$$

where

$$P_{UL} = P_{SR} + P_{RD} - P_{SR}P_{RD} \tag{4.15}$$

and

$$P_{DL} = P_{S_1R_1} + P_{R_1D_1} - P_{S_1R_1}P_{R_1D_1} \tag{4.16}$$

P_{UL} has already been derived in Chapter 3 i.e. product of $F_{\gamma_{SR}^f}(\gamma_{SR})$ and $F_{\gamma_{SR}^f}(\gamma_{SR})$. Now we have to calculate for P_{DL}. $P_{S_1R_1}$ is outage probability of satellite to HAPS link for which outage probability is negligible or almost zero due to negligible atmospheric affects in this region. $P_{R_1D_1}$ is outage probability of HAPS to GS in downlink. In this region, RF link is used for communication and its outage probability is given by (4.13). Finally , P_{DL} is nothing but $P_{R_1D_1}$ because $P_{S_1R_1} \approx 0$ By substituting corresponding values of P_{UL} and P_{DL} in (4.13), outage probability is obtained. The only change we can observe here compared to 4.4.1 is P_{UL} part, especially P_{SR}.

4.4.4 SER analysis of End-to-End Communication using FSO link with Single HAPS

The average SER of this system model is given by

$$P^e = P_{UL}^e + P_{DL}^e - P_{UL}^e P_{DL}^e \tag{4.17}$$

where

$$P_{UL}^e = P_{SR}^e + P_{RD}^e - P_{SR}^e P_{RD}^e \tag{4.18}$$

and

$$P_{DL}^e = P_{S_1R_1}^e + P_{R_1D_1}^e - P_{S_1R_1}^e P_{R_1D_1}^e \tag{4.19}$$

P_{UL}^e has already been derived in Chapter 2 and we have to calculate for downlink part i.e. P_{DL}^e. $P_{S_1R_1}^e$ is the average SER of satellite to HAPS link, which is average SER of AWGN channel due to reasons mentioned before and is given by

$$P_{S_1R_1}^e = \frac{A}{2}\mathrm{erfc}\left(\sqrt{\gamma_{avg}}B\right) \tag{4.20}$$

$P_{R_1D_1}^e$ is average SER for HAPS to GS link in which communication is done using RF link. Therefore, average SER of RF link is given by

$$P_{R_1D_1}^e = P_e^{rf} = \sum_{q=0}^{\infty} R_{1,q} \left[\frac{\mu(1+k)}{\gamma_{avg}}\right]^{-(\mu+q)} G_{2,2}^{2,1}\left(\frac{B^2\gamma_{avg}}{\mu(1+\kappa)} \left|\begin{array}{c} 1-q-\mu, 1 \\ 0, 0.5, - \end{array}\right.\right) \tag{4.21}$$

4.4.5 SER analysis of End-to-End Communication using FSO link with Multiple HAPS

The average SER of this system model is given by

$$P^e = P_{UL}^e + P_{DL}^e - P_{UL}^e P_{DL}^e \tag{4.22}$$

where

$$P_{UL}^e = P_{SR}^e + P_{RD}^e - P_{SR}^e P_{RD}^e \tag{4.23}$$

and

$$P_{DL}^e = P_{S_1R_1}^e + P_{R_1D_1}^e - P_{S_1R_1}^e P_{R_1D_1}^e \tag{4.24}$$

P_{UL}^e has already been derived in Chapter 2 and here, we have to calculate for downlink part i.e. P_{DL}^e. $P_{S_1R_1}^e$ is average SER of satellite to HAPS link, which is average SER of AWGN channel. Because of the atmospheric conditions in that region, FSO link acts as AWGN channel and it is given in (4.20). $P_{R_1D_1}^e$ is average SER of HAPS to GS link in which communication is done using RF link. Therefore, average SER of this link is average SER of RF link, which is given by (4.21).

4.4.6   SER analysis of End-to-End Communication using Hybrid Link

The average SER of this system model is given by

$$P^e = P^e_{UL} + P^e_{DL} - P^e_{UL}P^e_{DL} \tag{4.25}$$

where average SER for uplink is given by

$$P^e_{UL} = P^e_{SR} + P^e_{RD} - P^e_{SR}P^e_{RD} \tag{4.26}$$

and average SER for downlink is given by

$$P^e_{DL} = P^e_{S_1R_1} + P^e_{R_1D_1} - P^e_{S_1R_1}P^e_{R_1D_1} \tag{4.27}$$

P^e_{UL} has already been derived in Chapter 3 and here, we have to calculate for downlink part i.e. P^e_{DL}. $P^e_{S_1R_1}$ is the average SER of satellite to HAPS link, which is the average SER of AWGN channel and is given by (4.20). $P^e_{R_1D_1}$ is the average SER of HAPS to GS link in which communication is done using RF link. Therefore, average SER of RF link is given by (4.26).

4.5   Numerical Results and Discussions

In this section, we will analyze the derived closed-form expressions. We also demonstrate the effects of various parameters on outage probability and average SER. For numerical investigation, we set threshold SNR as γ_{th} = 5 dB, height of HAPS = 20km, $\lambda = 1.55\mu m$, $\alpha_{SR} = 2.89, \beta_{SR} = 2, \alpha_{RD} = 801.6, \beta_{RD} = 1024$ and parameters considered for making conclusions are pointing error coefficient, wind velocity and zenith angle. It is to be noted that E2E refers to end-to-end.
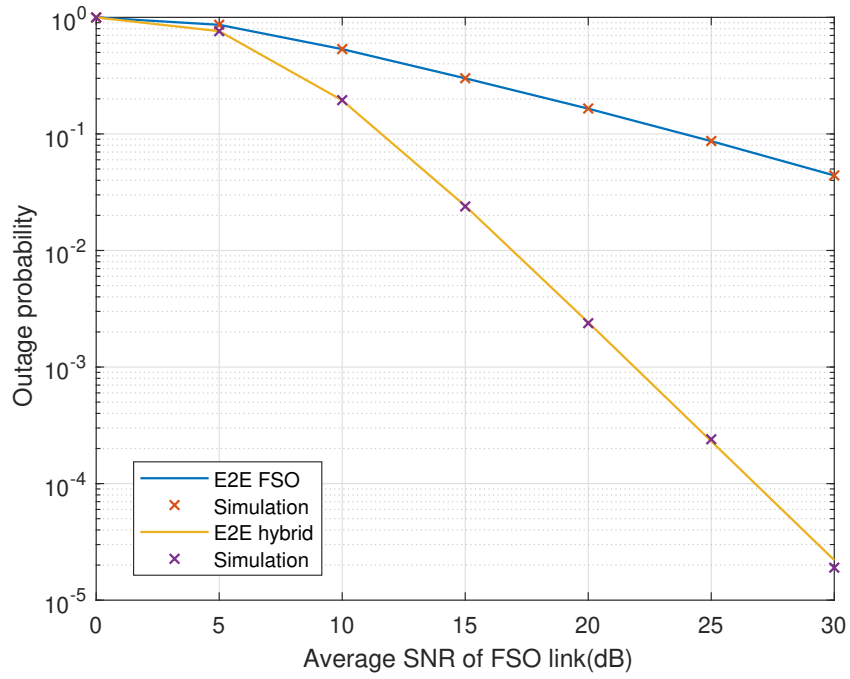
Figure 4.3: OP vs Avg SNR of FSO link for different system models

Figure 4.3 shows the comparison between two system models i.e. DH FSO and DH hybrid. We can clearly see that to achieve outage probability value of 10^{-1}, hybrid system requires average SNR of 12 dB and FSO system requires 24 dB. The SNR gain is 12 dB. We can conclude that hybrid system has better outage performance compared to FSO system .
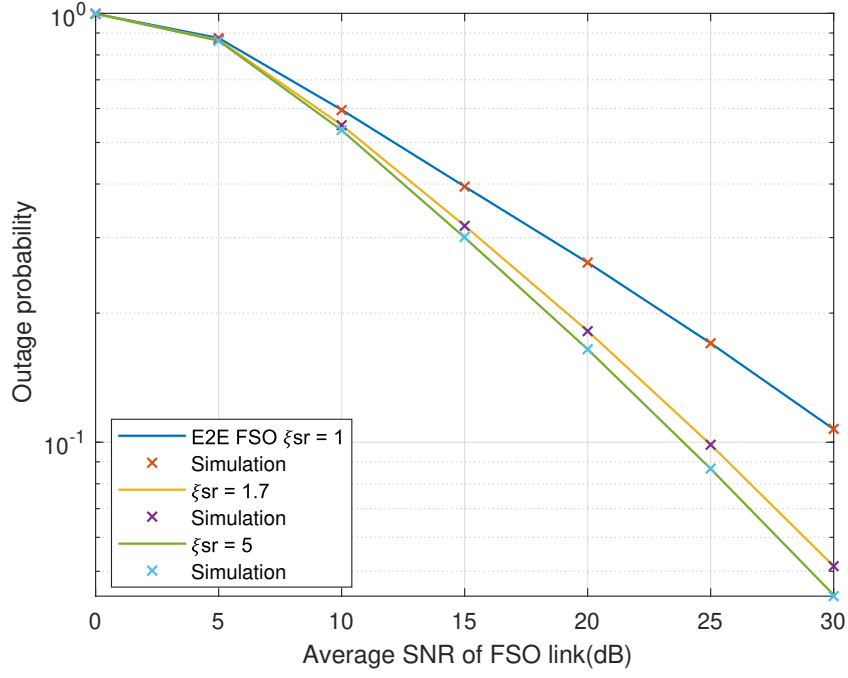
Figure 4.4: OP vs Avg SNR of FSO link for different values of ζ_{SR}

Figure 4.4 shows the effect of value of ζ_{SR} pointing error coefficient on the outage probability of the system model. From the plot, we can observe that the outage performance improves with increase in ζ_{SR}. Because, increase in pointing error coefficient implies decrease in pointing error. The SNRs required to achieve the outage probability of 10^{-2} for the system with $\zeta_{SR}=1$, $\zeta_{SR}=1.7$, $\zeta_{SR}=5$, are 30 dB, 25 dB, 24 dB, respectively. So, the SNR gains achieved by the system with $\zeta_{SR}=1$ w.r.t system with $\zeta_{SR}=1.7$, $\zeta_{SR}=5$ are 5 dB, 1 dB, respectively. Therefore, we can conclude that with the increase in value of ζ_{SR}, there is not much improvement in SNR gain.
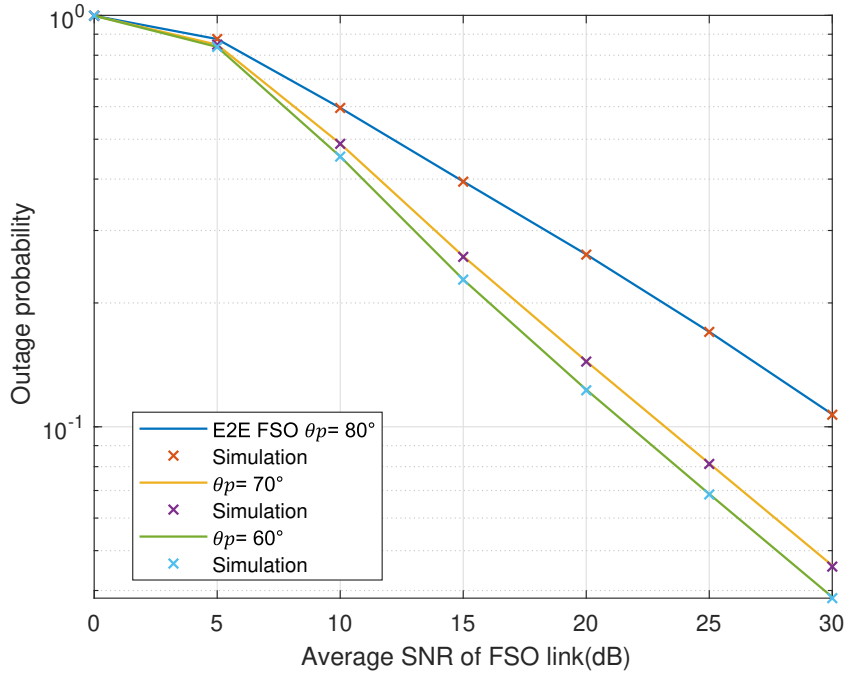
Figure 4.5: OP vs Avg SNR of FSO link for different values of θ_p
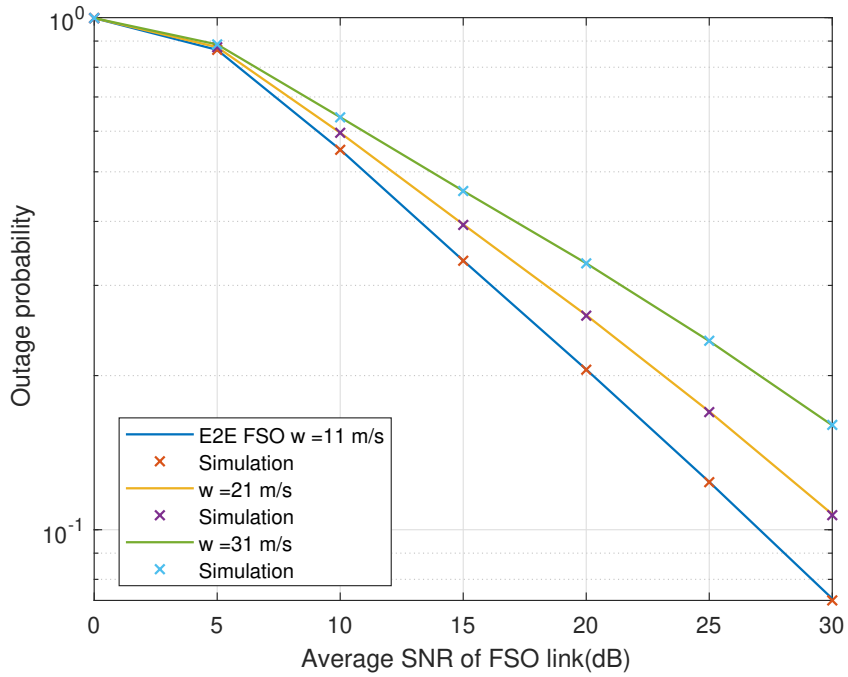

Figure 4.6: OP vs Avg SNR of FSO link for different values of w

Figure 4.5 and Figure 4.6 show the effect of the wind velocity and zenith angle on system model w.r.t outage probability. From both figures, we can observe that outage performance decreases with the increase in value of *w* and θ_p due to reasons mentioned before.

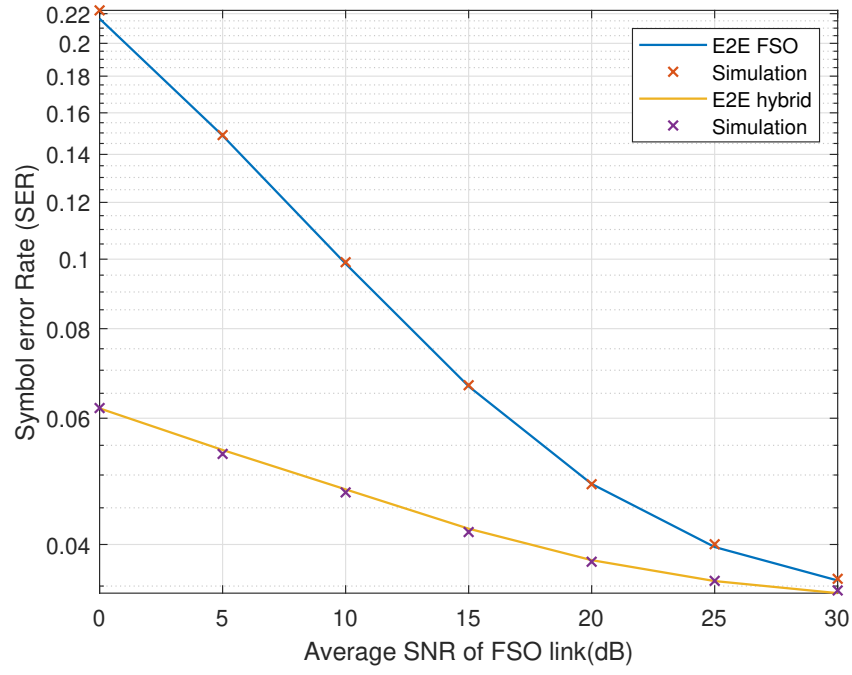Figure 4.7: SER vs. Avg SNR of FSO link for different system models

Figure 4.7 shows the comparison between two system models i.e. DH FSO and DH hybrid based on SER. We can clearly see that to achieve SER value of 0.05, hybrid system requires average SNR of 5 dB and FSO system requires 18 dB. The SNR gain is 13 dB. We can conclude that hybrid system has better SER performance compared to FSO system.
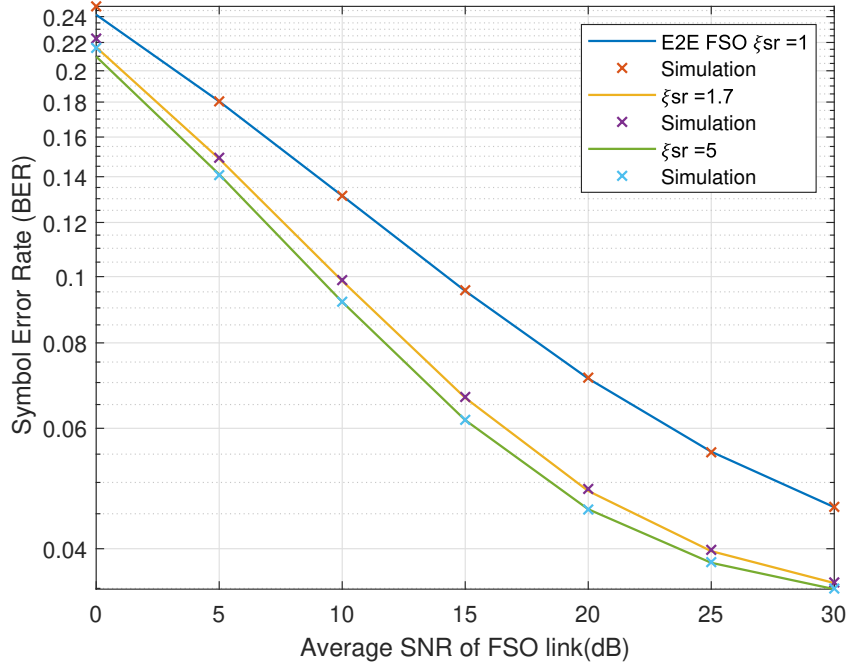
Figure 4.8: SER vs. Avg SNR of FSO link for different values of ξ_{sr}

Figure 4.8 shows the effect of value of pointing error coefficient ζ_{SR} on the SER performance. From the plot, we can observe that the SER improves with increase in ζ_{SR}. The SNRs required to achieve SER of 10^{-1} for the system with $\zeta_{SR}=1$, $\zeta_{SR}=1.7$, $\zeta_{SR}=5$ are 15 dB, 10 dB, 9 dB respectively. So, the SNR gains achieved by the system with $\zeta_{SR}=1$ w.r.t system with $\zeta_{SR}=1.7$, $\zeta_{SR}=5$ are 5 dB, 0.5 dB respectively. Therefore, we can conclude that with the increase in value of ζ_{SR}, there is not much improvement in SNR gain.
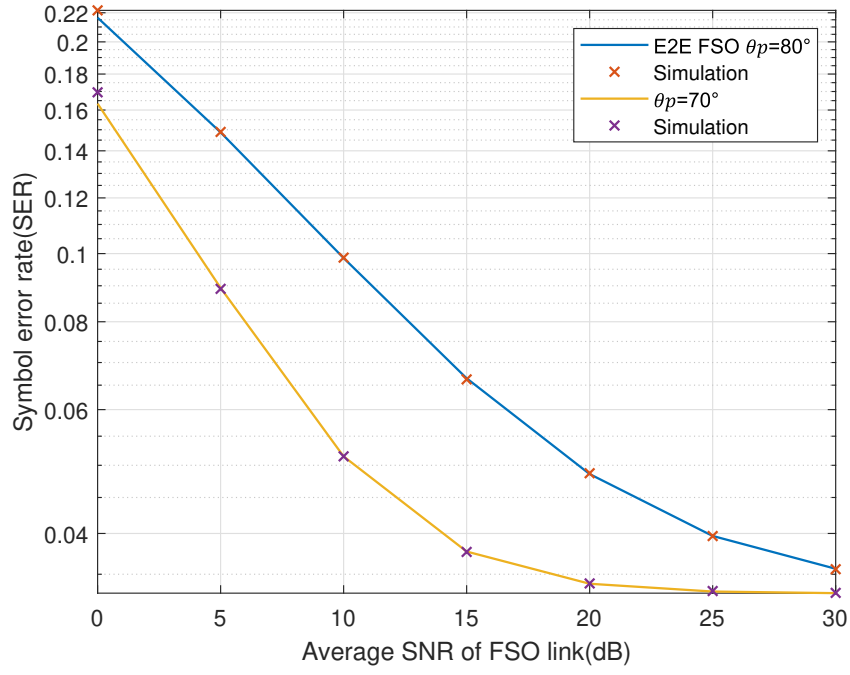
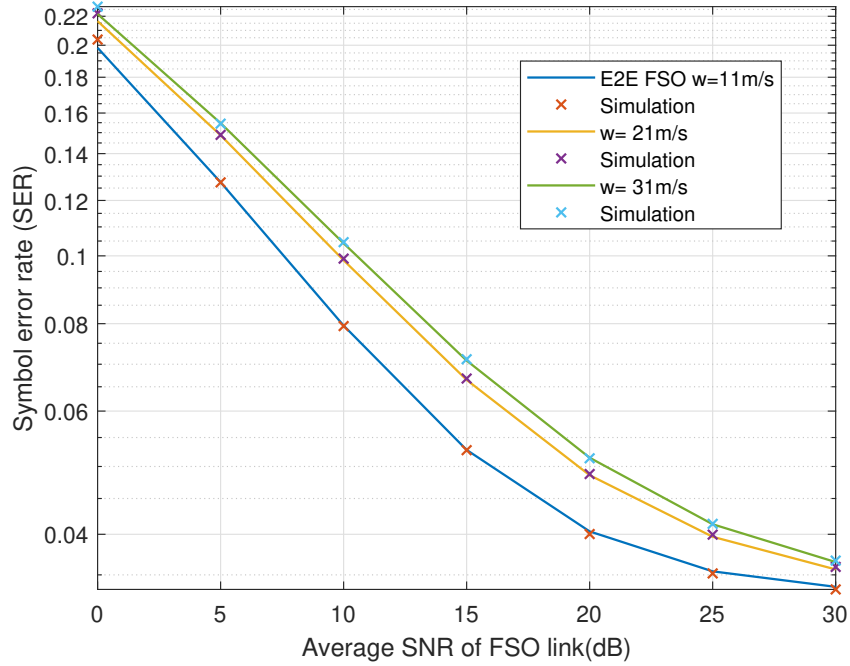Figure 4.9: SER vs Avg SNR of FSO link for different values of θ_p

Figure 4.10: SER vs Avg SNR of FSO link for different values of w

Figure 4.9 and Figure 4.10 show the effect of the wind velocity and zenith angle on system model w.r.t SER. From both figures, we can observe that SER decreases with the increase in value of w and θ_p due to the reasons mentioned before.

4.6 Conclusions

The performance of the end-to-end system model is examined in this chapter by deriving outage probability and SER expressions in closed-form over Malaga and shadowed $\kappa - \mu$ fading channels. In addition, MATLAB is used to compute the derived closed-form expressions. The outage performance of the proposed system model improves as the value of N increases, and the outage performance of the system with relay is better than the system without relay according to simulation results. Furthermore, it has been discovered that the hybrid system outperforms the FSO system. Finally, the theoretical outage probability and SER values accord well with the simulated outage probability and SER values acquired from Monte Carlo simulations.

Chapter 5

Conclusions and Future Work

This thesis examines the performance of the following three system models: uplink satellite communication using FSO link with HAPS as relay, uplink satellite communication using hybrid FSO/RF link between GS and HAPS, and end-to-end uplink and downlink satellite communication using HAPS. The analytical framework in this thesis has been carried out over Malaga fading channels for FSO link with pointing errors and shadowed $\kappa - \mu$ fading for RF link. The derived closed-form expressions for performance metrics are validated using Monte Carlo simulations.

5.1   Conclusions

In Chapter 2, we investigated the performance of the proposed satellite communication system model using FSO link with HAPS as relay. We considered multiple relays and employed PRS scheme to select the relay nodes. The closed-form expressions for performance measures like outage probability and average SER are derived and computed using MATLAB. The effect of the number of relays and other vital RF and FSO link parameters on the performance of the proposed system was revealed by numerical findings. In terms of outage probability and average SER, the proposed system outperforms the system without relay.

In Chapter 3, we investigated the performance of the proposed satellite communication system model using hybrid FSO/RF link for communication from GS to HAPS and FSO link for HAPS to satellite. We considered multiple relays and employed PRS scheme to select the relay nodes. Similarly, closed-form expressions for outage probability and average SER are derived and implemented using MATLAB. The effect of the number of relays and other

vital FSO and RF link parameters on the performance of the proposed system was revealed by numerical findings. In terms of outage probability and SER, system model in Chapter 3 outperforms the system model proposed in Chapter 2.

In Chapter 4, we investigated the performance of the end-to-end communication considering both uplink and downlink scenarios with multiple HAPS as relay nodes and we employ PRS scheme to select the best relay. In the first system model, FSO link is used for communication from GS to HAPS and in the second system model, hybrid FSO/RF link is used for communication from GS to HAPS. In the downlink scenario, we emply FSO link between satellite and HAPS as well as RF link between HAPS and GS. For both the system models, closed-form expressions for performance measures like outage probability and SER are derived and computed using MATLAB. In terms of outage probability and SER, our suggested hybrid system outperforms the FSO system. Also, the effect of the number of relays and other vital parameters on the performance of the proposed system models was revealed by numerical findings.

5.2 Future Works

The scope for the future work can be summarized as follows:

- Asymptotic expressions for average SER and ergodic capacity will be derived to gain more insights in terms of achievable capacity and diversity gain.

- Computation of ergodic capacity and outage capacity for multiple HAPS scenario.

- Generalization of SER expressions for N HAPS scenario considering FSO channel modelled using Malaga distribution.

- Computation of ergodic capacity and outage capacity for end-to-end system model.

Bibliography

[1]   Imran Ansari, Ferkan Yilmaz, and Mohamed-Slim Alouini. "Performance Analysis of FSO Links over Unified Gamma-Gamma Turbulence Channels". In: *IEEE Vehicular Technology Conference* 2015 (July 2015). DOI: 10.1109/VTCSpring.2015.7145999.

[2]   Imran Shafique Ansari, Ferkan Yilmaz, and Mohamed-Slim Alouini. "Performance Analysis of Free-Space Optical Links Over Málaga ($\mathcal{M}$) Turbulence Channels With Pointing Errors". In: *IEEE Transactions on Wireless Communications* 15.1 (2016), pp. 91–102. DOI: 10.1109/TWC.2015.2467386.

[3]   Ehsan Bayaki, Robert Schober, and Ranjan K Mallik. "Performance analysis of free-space optical systems in gamma-gamma fading". In: *IEEE GLOBECOM 2008-2008 IEEE Global Telecommunications Conference*. IEEE. 2008, pp. 1–6.

[4]   Ehsan Bayaki, Robert Schober, and Ranjan K Mallik. "Performance analysis of MIMO free-space optical systems in gamma-gamma fading". In: *IEEE Transactions on Communications* 57.11 (2009), pp. 3415–3424.

[5]   Manav R. Bhatnagar and M. K. Arti. "Performance Analysis of Hybrid Satellite-Terrestrial FSO Cooperative System". In: *IEEE Photonics Technology Letters* 25.22 (2013), pp. 2197–2200. DOI: 10.1109/LPT.2013.2282836.

[6]   Eylem Erdoğan et al. "Site Diversity in Downlink Optical Satellite Networks Through Ground Station Selection". In: (Oct. 2020).

[7]   I.S. Gradshteyn and I.M. Ryzhik. "Table of Integrals, Series, and Products". In: (2007). URL: http://fisica.ciens.ucv.ve/~svincenz/TISPISGIMR.pdf.

[8]   Mohammad Ali Khalighi and Murat Uysal. "Survey on Free Space Optical Communication: A Communication Theory Perspective". In: *IEEE Communications Surveys Tutorials* 16.4 (2014), pp. 2231–2258. DOI: 10.1109/COMST.2014.2329501.

[9]   Mi Li et al. "Investigation on the UAV-To-Satellite Optical Communication Systems". In: *IEEE J.Sel. A. Commun.* 36.9 (Sept. 2018), pp. 2128–2138. ISSN: 0733-8716. DOI: 10.1109/JSAC.2018.2864419. URL: https://doi.org/10.1109/JSAC.2018.2864419.

[10]   Jiajia Liu et al. "Space-air-ground integrated network: A survey". In: *IEEE Communications Surveys & Tutorials* 20.4 (2018), pp. 2714–2741.

[11]   *MeijerG*. Accessed: 25-May-2022. Wolfram Research. 1996. URL: https://reference.wolfram.com/language/ref/MeijerG.html.

[12]   Swaminathan R et al. "HAPS-Based Relaying for Integrated Space–Air–Ground Networks With Hybrid FSO/RF Communication: A Performance Analysis". In: *IEEE Transactions on Aerospace and Electronic Systems* 57.3 (2021), pp. 1581–1599. DOI: 10.1109/TAES.2021.3050663.

[13]   Swaminathan Ramabadran, George Karagiannidis, and Rajarshi Roy. "Joint Antenna and Relay Selection Strategies for Decode-and-Forward Relay Networks". In: *IEEE Transactions on Vehicular Technology* 65 (Nov. 2016), pp. 9041–9056. DOI: 10.1109/TVT.2016.2515265.

[14]   Suyash Shah et al. "Adaptive-combining-based hybrid FSO/RF satellite communication with and without HAPS". In: *IEEE Access* 9 (2021), pp. 81492–81511.

[15]   Shubha Sharma, AS Madhukumar, and Swaminathan R. "MIMO Hybrid FSO/RF System Over Generalized Fading Channels". In: *IEEE Transactions on Vehicular Technology* 70.11 (2021), pp. 11565–11581. DOI: 10.1109/TVT.2021.3111401.

[16]   Shubha Sharma et al. "Switching-Based Transmit Antenna/Aperture Selection in a MISO Hybrid FSO/RF System". In: (2018), pp. 1–6. DOI: 10.1109/GLOCOM.2018.8647284. URL: https://doi.org/10.1109/GLOCOM.2018.8647284.

[17]   Shubha Sharma et al. "Switching-based transmit antenna/aperture selection in a MISO hybrid FSO/RF system". In: *2018 IEEE Global Communications Conference (GLOBECOM)*. IEEE. 2018, pp. 1–6.

[18]   Muneer Usman, Hong-Chuan Yang, and Mohamed-Slim Alouini. "Practical Switching-Based Hybrid FSO/RF Transmission and Its Performance Analysis". In: *IEEE Photonics Journal* 6.5 (2014), pp. 1–13. DOI: 10.1109/JPHOT.2014.2352629.

[19]   Narendra Vishwakarma and R Swaminathan. "Performance analysis of hybrid FSO/RF communication over generalized fading models". In: *Optics Communications* 487 (2021), p. 126796.

[20]   Mathuranathan Viswanathan. "Simulation of digital communication systems using Matlab". In: *Mathuranathan Viswanathan at Smashwords* (2013).

[21]   Olfa Ben Yahia, Eylem Erdogan, and Gunes Karabulut Kurt. "On the Performance of HAPS-assisted Hybrid RF-FSO Multicast Communication Systems". In: *arXiv preprint arXiv:2109.10131* (2021).

[22]   Olfa Ben Yahia et al. "HAPS selection for hybrid RF/FSO satellite networks". In: *arXiv preprint arXiv:2107.12638* (2021).